



Discovery of novel quinoline-based mTOR inhibitors via introducing intra-molecular hydrogen bonding scaffold (iMHBS): The design, synthesis and biological evaluation



Xiaodong Ma, Xiaoqing Lv, Ni Qiu, Bo Yang, Qiaojun He, Yongzhou Hu*

Zhejiang Province Key Laboratory of Anti-Cancer Drug Research, College of Pharmaceutical Sciences, Zhejiang University, Hangzhou 310058, China

ARTICLE INFO

Article history:

Received 11 September 2015

Revised 26 October 2015

Accepted 4 November 2015

Available online 4 November 2015

Keywords:

Quinoline derivatives

mTOR inhibitor

Anti-proliferative efficacy

Selectivity

Negative feedback loop

Stability

ABSTRACT

A series of quinoline derivatives featuring the novelty of introducing intra-molecular hydrogen bonding scaffold (iMHBS) were designed, synthesized and biologically evaluated for their mTOR inhibitory activity, as well as anti-proliferative efficacies against HCT-116, PC-3 and MCF-7 cell lines. As a result, six compounds exhibited significant inhibition against mTOR with IC₅₀ values below 35 nM. Compound **15a**, the most potent mTOR inhibitor reported herein (IC₅₀ = 14 nM), also displayed the most favorable cellular activities, with the IC₅₀ values of 0.46, 0.61 and 0.24 μM against HCT-116, PC-3 and MCF-7, respectively. Besides, several compounds in this series were identified to be selective over class I PI3Ks. Further western blot analysis of **16b**, a representative compound in this series, highlighted their advantage in surmounting the S6K/IRS1/PI3K negative feedback loop upon dual inhibition of mTORC1 and mTORC2. In addition to the remarkable activity, **15a** demonstrated acceptable stability in simulated gastric fluid (SGF), simulated intestinal fluid (SIF) and liver microsome, thereby being valuable for extensive in vivo investigation.

© 2015 Elsevier Ltd. All rights reserved.

1. Introduction

Nowadays, the medicinal potential of the mammalian target of rapamycin (mTOR), a key node of PI3K/Akt/mTOR cascade, has been validated by several rapalogues (rapamycin and its semi-synthetic analogs) prescribed for cancer treatment in clinic.¹ In cells, mTOR assembles into two functionally distinct multi-protein complexes, known as mTORC1 and mTORC2.² While mTORC1 locates downstream of Akt, serving as a crucial regulator of translation and cell proliferation, mTORC2 resides upstream of Akt,³ activating it upon phosphorylation on Ser473. Rapalogues, such as rapamycin, everolimus and temsirolimus, selectively suppress the activity of mTORC1 through an allosteric mechanism. However, the inhibition is partial due to the failure in attenuating the kinase activity of mTOR.⁴ In addition, rapalogues rarely interfere with the activity of mTORC2, except in a small subset of cell lines.⁵ More importantly, the rapalogue treatment releases the S6K/IRS1/PI3K negative feedback loop, which consequently upregulates Akt and undermines the anti-proliferative efficacy of mTORC1 inhibition.⁶ With these shortcomings, the application of allosteric mTOR inhibitors has been confined to a limited number of tumor types.^{7–9} In compar-

ison, ATP-competitive mTOR modulators (mTOR kinase inhibitors) simultaneously inhibiting mTORC1 and mTORC2 may conquer the hyperactivation of Akt induced by the negative feedback loop, hence broadening anti-tumor spectrum and improving therapeutic efficacy.^{7,10}

Throughout the past decade, numerous ATP-competitive mTOR inhibitors have been advanced into clinical trial, including mTOR selective (AZD-2014,^{11,12} MLN-0128¹³) and dual mTOR/PI3K inhibitors (BEZ-235,^{14–16} GSK-2126458,¹⁷ XL-765,^{18,19} PF-04691502,²⁰ etc.). During the pursuit of ATP-competitive mTOR inhibitors, Torin 2 (Fig. 1) inspired our interest by virtue of its remarkable mTOR inhibitory activity and structural differentiation from other molecules belonging to this class. Despite its favorable bioavailability and overall exposure, Torin 2 displayed a short elimination half-life of 0.72 h following oral administration.¹⁰ Besides, a majority of analogs sharing the same benzonaphthridinone core as Torin 2 also suffered from poor PK profiles due to the instability in liver microsome and limited solubility.²¹

According to our insight into the binding mode of Torin 2 with mTOR,²² the N1 of the quinoline conferred a critical H-bond contact to residue Val2240 in the hinge region. Meanwhile, the amino pyridine moiety of Torin 2 was projected into the inner hydrophobic pocket of mTOR catalytic cleft. The α,β-unsaturated lactam fused to the C-3 and C-4 positions of quinoline was important for constraining the pendant phenyl ring to the bioactive conformation,

* Corresponding author. Tel./fax: +86 571 88208460.

E-mail address: huyz@zju.edu.cn (Y. Hu).

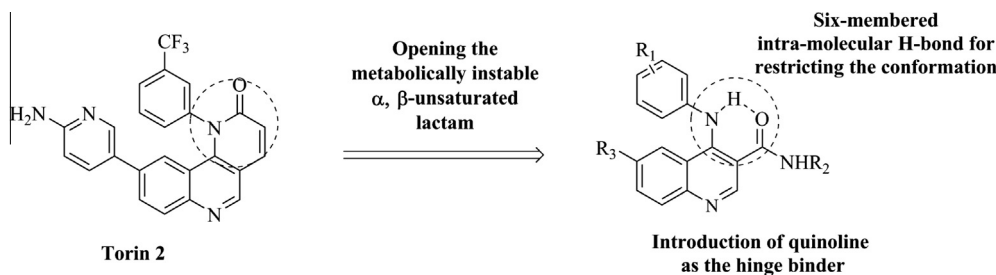


Figure 1. The design rationale for the quinoline derivatives with iMHBS.

in which the trifluoromethyl group packed into an *N*-lobe pocket. However, as Michael-acceptor, the α,β -unsaturated lactam was liable to be captured in vivo, thereby accounting for the short elimination half-life of Torin 2. Considering this, our optimization prioritized obviating the metabolically instable α,β -unsaturated lactam and introducing an intra-molecular H-bond to mimic it. Accordingly, a series of quinoline derivatives were designed via a de-construction approach to break the lactam of Torin 2 (Fig. 1). These quinolines were characterized by a C-3 amide functionality and a C-4 substituted aniline, upon which a pseudo-ring was desired to form between the amide oxygen and the secondary amine hydrogen through a six-membered intra-molecular H-bond.

We envisioned this type of intra-molecular hydrogen bonding scaffold (iMHBS) not only restricted the basic conformation of Torin 2, but also eliminated the metabolically susceptible site. Besides, another advantage of the iMHBS designed herein lay in the reduced ring members compared to Torin 2, thereby being beneficial for improving the solubility. This research was focused on the preparation, in vitro evaluation, as well as structure–activity relationship (SAR) study of these quinolines to validate the iMHBS strategy and screen promising compounds for further development.

2. Results and discussion

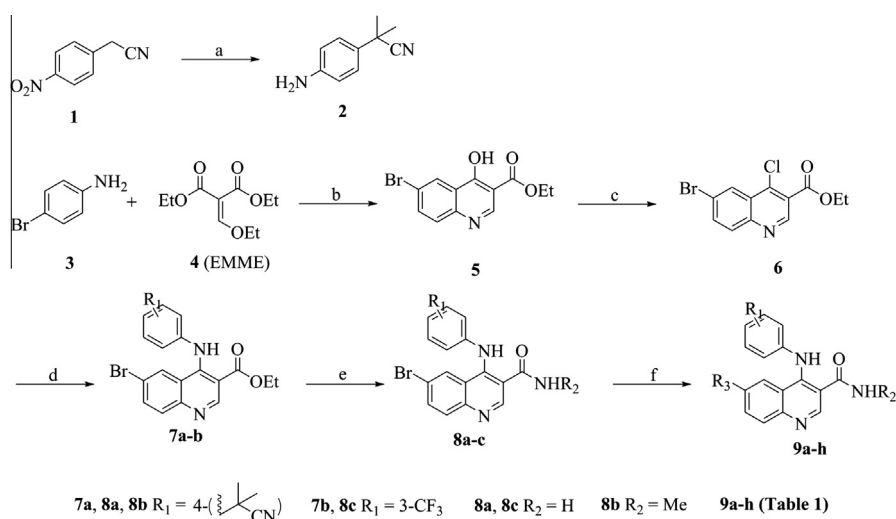
2.1. Chemistry

The synthetic route for compounds **9a–h** was outlined in Scheme 1. Firstly, 4-nitrophenylacetonitrile **1** was subjected to

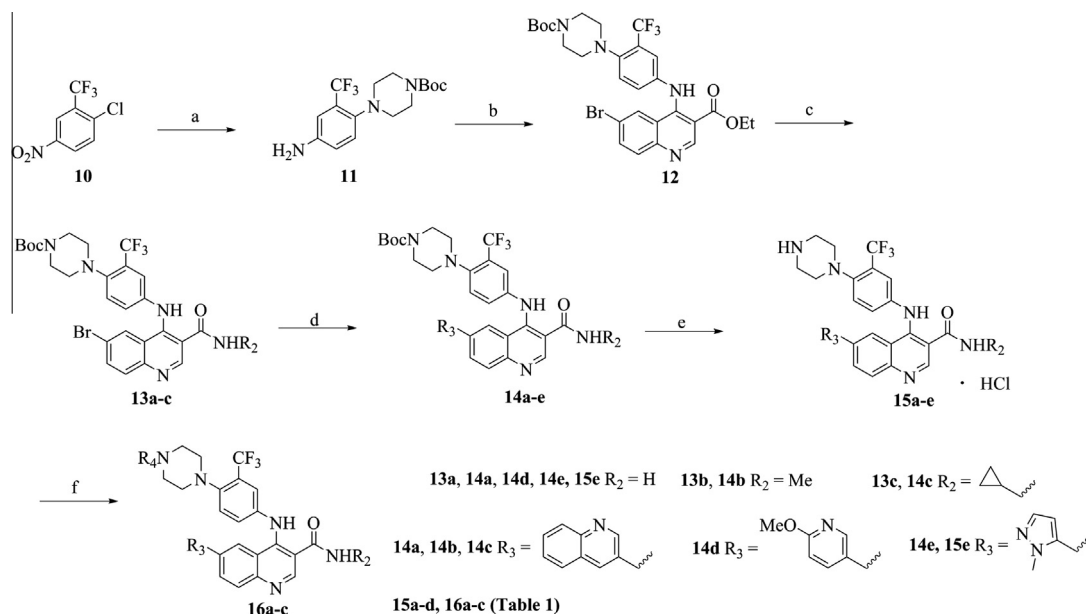
di-methylation at the benzyl position and catalytic hydrogenation to afford the substituted aniline **2**. According to the procedure reported in the literature,²³ condensation of 4-bromoaniline **3** with diethyl ethoxymethylenemalonate **4** (EMME), followed by the intra-molecular cyclization, provided the quinoline derivative **5**. Afterwards, treatment of **5** with POCl₃ gave the C-4 chlorine quinoline derivative **6**, which experienced SNAr reaction with corresponding substituted aniline to furnish intermediates **7a** and **7b**. Subsequent aminolysis converted the C-3 ester moiety of **7a** or **7b** into corresponding amide functionality. The newly formed **8a–c** finally underwent Suzuki coupling with corresponding borate to generate target compounds **9a–h**.

The preparation of compounds bearing C-4 elongated substructure was displayed in Scheme 2. SNAr reaction of *N*-Boc-piperazine with **10** and the following catalytic hydrogenation provided **11** as an important fragment. It was then subjected to SNAr reaction with **6** to afford the intermediate **12**. After a sequence of aminolysis, Suzuki coupling and removal of the Boc-protecting group, target compounds **15a–d** and intermediate **15e** were obtained as the hydrochlorides. Further acylation or sulfonylation at the piperazine furnished target compounds **16a–c**.

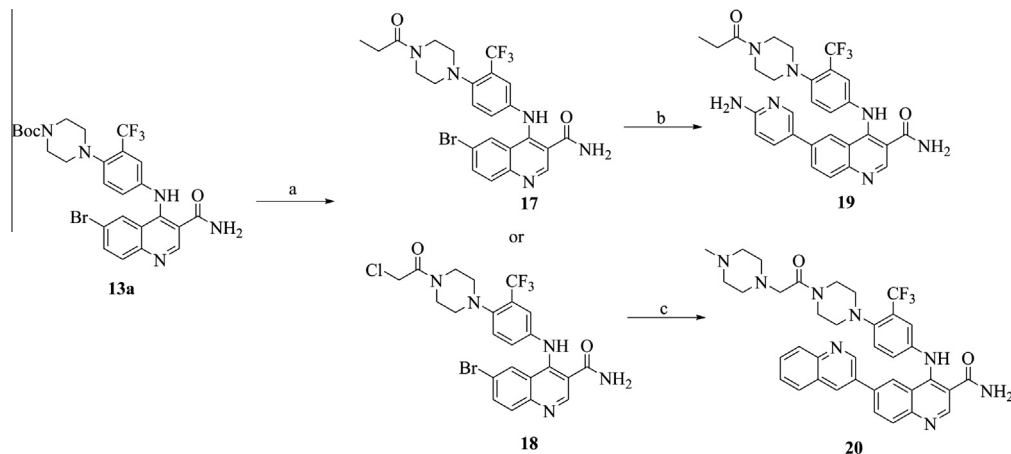
As shown in Scheme 3, compound **19** was obtained via removal of the Boc-protecting group, propionylation and subsequent Suzuki coupling upon utilization of **13a** as the starting material. After removing the Boc-protecting group of **13a**, the newly formed product was treated with chloroacetyl chloride to give **18** as an intermediate. It was then subjected to nucleophilic attack by *N*-methyl piperazine and Suzuki coupling with corresponding borate to furnish **20** as the target compound.



Scheme 1. Reagents and conditions: (a) (1) MeI, TBAB, DCM/H₂O, rt; (2) H₂, Pd/C, MeOH, rt; (b) (1) 80 °C; (2) Ph₂O, 250 °C; (c) DMF, POCl₃, reflux; (d) **2** or 3-trifluoromethylaniline, AcONa, HAc, rt; (e) NH₃ (EtOH solution, concentrated) or MeNH₂ (EtOH solution, concentrated), 80 °C; (f) corresponding borate, K₂CO₃, Pd(PPh₃)₄, H₂O/1,4-dioxane, 100 °C.



Scheme 2. Reagents and conditions: (a) (1) *N*-Boc-piperazine, K_2CO_3 , DMF, 40 °C; (2) H_2 , Pd/C, MeOH, rt; (b) **6**, AcONa, HAc, rt; (c) NH_3 (EtOH solution, concentrated), $MeNH_2$ (EtOH solution, concentrated) or cyclopropylamine, 80 °C; (d) corresponding borate, K_2CO_3 , Pd(PPh_3)₄, $H_2O/1,4$ -dioxane, 100 °C; (e) HCl (EtOAc solution, concentrated), 0 °C to rt; (f) Et_3N , AcCl or MsCl, THF, 0 °C.



Scheme 3. Reagents and conditions: (a) (1) TFA, DCM, 0 °C to rt; (2) Et_3N , propionyl chloride or chloroacetyl chloride, THF, 0 °C to rt; (b) corresponding borate, K_2CO_3 , Pd(PPh_3)₄, $H_2O/1,4$ -dioxane, 100 °C; (c) (1) *N*-methyl piperazine, K_2CO_3 , CH_3CN , 80 °C; (2) corresponding borate, K_2CO_3 , Pd(PPh_3)₄, $H_2O/1,4$ -dioxane, 100 °C.

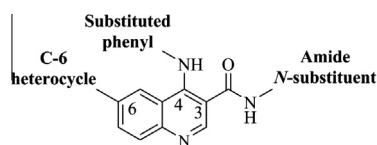
2.2. mTOR inhibitory activity

All the target compounds were evaluated for their inhibitory activity against mTOR via lance ultra assay with PI-103, an mTOR/PI3K dual inhibitor, as the positive control. According to the results summarized in Table 1, nearly half of them (**9b**, **9d**, **9g**, **15a**, **16b**, **16c**, **19** and **20**) exhibited remarkable inhibition against mTOR with IC_{50} values at two-digit nanomolar level. In particular, six quinoline derivatives, including **9b**, **9d**, **15a**, **16b**, **19** and **20**, displayed comparable mTOR inhibitory activity to PI-103 with IC_{50} values lower than 35 nM.

From the data for mTOR inhibition, some valuable SARs can be deduced. As for the C-3 amide functionality, introduction of *N*-substituent was detrimental for activity. For example, compounds **9c**, **9e** and **15b** bearing a methyl substituent at the nitrogen demonstrated significantly compromised activity compared to corresponding *N*-unsubstituted counterparts **9b**, **9d** and **15a**. With the *N*-substituent being bulkier, the activity decreased sharply.

Replacement of the methyl group with cyclopropyl resulted in a further loss in activity, as illustrated by the activity of **15c** versus **15b**. Additionally, C-6 heterocycle served as another critical factor to affect activity, with aminopyridine or quinoline more beneficial than methoxy pyridine or *N*-methyl pyrazole. Compounds **9f** and **15d**, both featuring a C-6 methoxy pyridine moiety, were approximately 20-fold less potent than corresponding aminopyridine derivative **9d** and quinoline derivative **15a**. Similarly, neither the C-6 *N*-methyl pyrazole derivative **9a** nor **16a** exhibited favorable activity as respective aminopyridine counterpart **9d** and quinoline counterpart **16c** did. In comparison, alteration in C-4 aniline only had a slight impact on activity of these compounds, as exemplified by the C-6 aminopyridine derivatives **9d**, **9g** and **19**. Despite varied substitution on the aniline, they displayed comparable mTOR inhibitory activity with IC_{50} values being 30, 51 and 21 nM, respectively. Besides, further derivatization at the piperazine failed to enhance potency, according to the data of compounds **15a**, **16b** and **20**.

Table 1
In vitro biological activities of the target quinoline derivatives



Compd	Substituted phenyl	C-6 heterocycle	Amide N-substituent	mTOR (IC ₅₀ , nM)	HCT-116 (IC ₅₀ , μM)	PC-3 (IC ₅₀ , μM)	MCF-7 (IC ₅₀ , μM)
9a			H	1105	17.26	>50	1.25
9b			H	33	4.56	2.82	0.95
9c			Me	514	8.73	7.12	1.30
9d			H	30	0.67	0.83	0.52
9e			Me	280	4.66	1.74	0.49
9f			H	674	2.57	1.66	1.58
9g			H	51	1.83	1.08	0.41
9h			H	361	3.17	6.39	0.60
15a			H	14	0.46	0.61	0.24
15b			Me	806	a	a	a
15c				>3000	a	a	a
15d			H	284	2.05	0.99	0.78
16a			H	1225	14.71	7.08	2.69
16b			H	31	1.29	3.90	0.44
16c			H	73	1.00	3.73	0.36
19			H	21	2.40	1.46	0.57
20			H	24	0.97	0.99	0.44
PI-103				16			
BEZ-235				21 ^b	0.20	0.21	0.05

^a Not identified.

^b IC₅₀ value reported in the literature.

2.3. Anti-proliferative activity

Encouraged by the favorable enzymatic activity of the prepared quinoline derivatives, we subsequently evaluated their anti-proliferative efficacies against several human tumor cell lines, including HCT-116, PC-3 and MCF-7. BEZ-235, an mTOR/PI3K dual inhibitor

under phase II clinical trial, was employed as the positive control. On the whole, compounds with two-digit nanomolar mTOR inhibitory activity (**9b**, **9d**, **9g**, **15a**, **16b**, **16c**, **19** and **20**) also demonstrated attractive potency against all the tested cell lines. As shown in **Table 1**, the IC₅₀ values were at low micromolar or sub-micromolar level without exception. Among them, **15a**, the most

remarkable mTOR inhibitor in this series, exhibited the most favorable cellular activities as well with IC₅₀ values of 0.46, 0.61 and 0.24 μM against HCT-116, PC-3 and MCF-7, respectively. Besides, **9d** also displayed distinguished efficacy against all the three cell lines with IC₅₀ values at submicromolar level. Throughout the tested cell lines, MCF-7 was regarded to be the most susceptible to these quinoline derivatives. Against the cell line, six compounds exhibited IC₅₀ values below 0.5 μM, and the other ones showed IC₅₀ values lower than 3.0 μM.

2.4. Selectivity over class I PI3Ks

Compounds **9b**, **15a** and **16b** in this series were further evaluated for their inhibitory activities against PI3Kα, PI3Kβ, PI3Kγ and PI3Kδ with PI-103 as the positive control. As summarized in Table 2, none of them displayed significant inhibition against the four class I PI3Ks at the concentration of 1.0 μM. Thereby, **9b**, **15a** and **16b**, as potent mTOR inhibitors, simultaneously exhibited acceptable specificity over class I PI3Ks.

2.5. Western blot analysis

To highlight the merits of mTOR kinase inhibitors, **16b**, as a representative of this series, was further investigated for its potential to obviate the S6K/IRS1/PI3K negative feedback loop via western blot analysis in MCF-7 cell line (Fig. 2). Herein, pAKT(Ser473) served as the biomarker for inhibition of mTORC2, while pS6(Ser235) was an indicator for suppression of mTORC1. As a consequence, BEZ-235 and **16b** induced a remarkable downregulation of both pAKT(Ser473) and pS6(Ser235) at 0.5 μM. Particularly, a complete downregulation of pAKT(Ser473) was accomplished by **16b** at the concentration as low as 0.1 μM. The simultaneous inhibition

of mTORC1 and mTORC2 therefore provided a powerful evidence for the capability to prevent the feedback loop upon **16b** treatment. On the contrary, rapamycin failed to downregulate pAKT(Ser473) despite the decrease in the level of pS6(Ser235) at 0.5 μM. Instead, rapamycin treatment culminated in the upregulation of pAKT(Ser473), which indicated the release of the negative feedback loop.

2.6. In vitro stability

To direct the in vivo development of these quinoline derivatives, **15a** was then evaluated for its stability in simulated gastric fluid (SGF), simulated intestinal fluid (SIF) and liver microsome. As a result, almost no degradation was observed upon incubation of this compound in both SGF and SIF after 45 min. Besides, it demonstrated acceptable stability in rat liver microsome (RLM) with nearly 50% left at 30 min. Meanwhile, favorable stability was exhibited by **15a** in human liver microsome (HLM) with 80% and 73% remaining at 30 min and 60 min, respectively.

2.7. Molecular docking

For probing the possible binding mode of these quinoline derivatives, compound **15a** was docked into the mTOR catalytic cleft based on the cocrystal structure of Torin 2 complexed with mTOR. According to Figure 3a and b, the nitrogen of quinoline template and C-3 amide hydrogen engaged in two H-bonds with the critical residue Val2240 in hinge region. Meanwhile, the hydroxyl of residue Tyr2225 that locating at the inner hydrophobic pocket served as an H-bond donor for the quinoline at the C-6 position of quinoline core. In addition to these H-bond interactions, the quinoline template made a π–π contact to the indole moiety of Trp2239, which was also observed in the cocrystal structure of Torin 2 complexed with mTOR. As formerly hypothesized, the C-3 amide oxygen and C-4 secondary amine hydrogen were within H-bond distance and the intra-molecular H-bond formed between them restricted the orientation of the C-4 substituted aniline. In this conformation, the trifluoromethyl group packed into the N-lobe pocket (Leu2185, Pro 2169, etc.). As for compound **15b**, however, the N-methyl amide moiety at the C-3 position had to rotate away from the indole of Trp2239 for obviating the unfavorable contact (Fig. 3c). Consequently, the H-bond interaction with Val2240 was weakened and the H-bond contact to Tyr2225 decreased due to the concerted movement of the quinoline core, which accounted for the compromised activity of **15b**.

Table 2
The inhibitory activities of compounds **9b**, **15a** and **16b** against class I PI3Ks

Compd	PI3Kα	PI3Kβ	PI3Kγ	PI3Kδ
9b	26.9% ^a	10.3% ^a	–2.4% ^a	–12.8% ^a
15a	32.3% ^a	1.0% ^a	6.7% ^a	16.7% ^a
16b	2427 ^b	>5000 ^b	939 ^b	>5000 ^b
PI-103	12 ^b	13 ^b	48 ^b	10 ^b

^a Inhibition rate at 1.0 μM.

^b IC₅₀ value (nM).

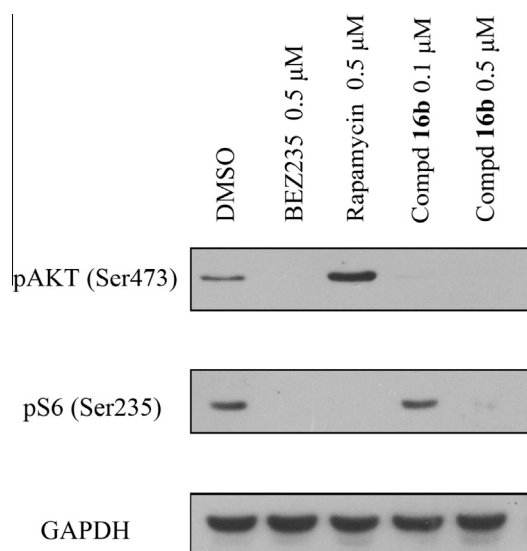


Figure 2. Western blot analysis of the quinoline derivative **16b** in MCF-7 cell line.

3. Conclusion

Built upon our insight into the cocrystal structure of Torin 2 complexed with mTOR, a novel structural series of quinoline derivatives were obtained via introducing iMHBS to mimic the bioactive conformation of Torin 2. All the target quinolines were evaluated for their mTOR inhibitory activity and the majority were tested for the anti-proliferative efficacies against HCT-116, PC-3, as well as MCF-7 cell lines. In general, the quinolines with two-digit nanomolar mTOR inhibitory activity, namely **9b**, **9d**, **9g**, **15a**, **16b**, **16c**, **19** and **20**, also demonstrated attractive potency against all the tested cell lines. In particular, compound **15a**, the most potent mTOR inhibitor in this series (IC₅₀ = 14 nM), simultaneously displayed the most favorable cellular activities, with respective IC₅₀ value of 0.46, 0.61 and 0.24 μM against HCT-116, PC-3 and MCF-7. Besides, several compounds in this series, including **9b**, **15a** and **16b**, were identified to be selective over class I PI3Ks. The advantage of these mTOR kinase inhibitors over rapalogues was further validated by western blot analysis in MCF-7 cell line, which

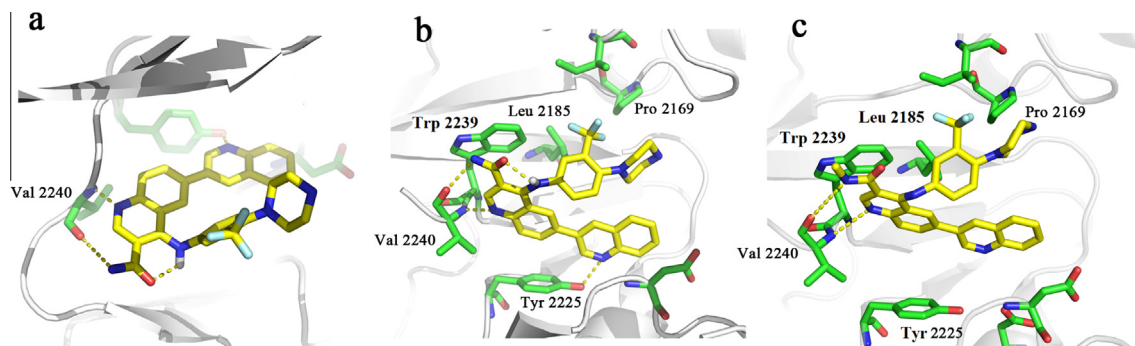


Figure 3. Molecular docking of quinoline derivatives **15a** (a and b) and **15b** (c) into the catalytic cleft of mTOR.

highlighted the capability of **16b**, a representative in this series, to conquer the S6K/IRS1/PI3K negative feedback loop upon the inhibition of both mTOR complexes. Moreover, **15a** showed acceptable gastrointestinal and liver microsomal stability in vitro, thereby meriting extensive in vivo investigation.

4. Experimental

4.1. Chemistry

The reagents and solvents for reaction were purchased from common commercial suppliers. If necessary, purification was carried out prior to use. Melting points were uncorrected and determined on a Büchi B-540 apparatus (Büchi Labortechnik, Flawil, Switzerland). ^1H NMR and ^{13}C NMR spectra were recorded on 500 MHz and 125 MHz instruments (Bruker Bioscience, Billerica, MA, USA), respectively, with tetramethylsilane (TMS) as internal standard. ESI mass spectral data were obtained by Esquire-LC-00075 spectrometer (Bruker Bioscience). Flash column chromatography was performed using silica gel (200–300 mesh). HPLC was performed using an Agilent 1200 system with UV detection at 254 nm, eluting with a binary solvent system A and B or C and B [A: H_2O ; B: CH_3OH ; C: H_2O with 0.12% ammonium acetate (W/V)]. Analytical purity of all compounds was >95% unless stated otherwise.

4.1.1. 2-(4-Aminophenyl)-2-methylpropanenitrile (**2**)

To a suspension of 4-nitrophenylacetonitrile **1** (1.0 equiv, 4.50 g, 27.8 mmol), tetrabutyl ammonium bromide (TBAB, 0.448 g, 1.39 mmol, 0.05 equiv) and iodomethane (11.8 g, 83.4 mmol, 3.0 equiv) in dichloromethane (DCM, 40.0 mL) was added sodium hydroxide (2.78 g, 69.5 mmol, 2.5 equiv) in water (40.0 mL) dropwise. After stirring at room temperature for 8 h, the organic layer was separated, washed with brine, dried with anhydrous Na_2SO_4 and concentrated in vacuo. Then the residue was subjected to flash column chromatography using EA/PE (1:14–1:7) as eluent to furnish the di-methylated product as a white crystal. Yield: 83%; ESI-MS: $m/z = 191$ $[\text{M}+\text{H}]^+$. The di-methylated product (4.38 g, 23.1 mmol) and 10% Pd/C (10% of the substrate, w/w) were shaken in methanol (60.0 mL) and the mixture was stirred at room temperature under H_2 (balloon) atmosphere overnight. After this time, Pd/C was filtered and the filtrate was concentrated in vacuo to provide **2** as a colorless oil, which slowly solidified and was used for the next step without purification. Yield: 95%. ESI-MS: $m/z = 161$ $[\text{M}+\text{H}]^+$.

4.1.2. Ethyl 6-bromo-4-hydroxyquinoline-3-carboxylate (**5**)

A mixture of 4-bromoaniline **3** (10.0 g, 58.48 mmol, 1.0 equiv) with diethyl ethoxymethylenemalonate **4** (EMME, 12.63 g, 58.48 mmol, 1.0 equiv) was warmed in oil bath at 80°C for 2 h.

Subsequently, ethanol formed during the reaction was removed under reduced pressure and diphenyl ether (50 mL) was added to the resultant white solid. After being heated at 250°C for 6 h, the mixture was cooled and petroleum ether (PE, 50 mL) was added. The precipitated product was collected, washed successively with PE and EtOAc, and dried in vacuo to give the intermediate as a white solid. Yield: 61%; ^1H NMR (500 MHz, $\text{DMSO}-d_6$): δ 12.46 (s, 1H, OH), 8.60 (s, 1H, Ar-H), 8.23 (d, 2.5 Hz, 1H, Ar-H), 7.88 (dd, 8.5 Hz, 2.5 Hz, 1H, Ar-H), 7.61 (d, 8.5 Hz, 1H, Ar-H), 4.23 (q, 7.0 Hz, 2H, CH_2), 1.29 (t, 7.0 Hz, 3H, CH_3). ESI-MS: $m/z = 296$ $[\text{M}+\text{H}]^+$; $m/z = 294$ $[\text{M}-\text{H}]^-$.

4.1.3. Ethyl 6-bromo-4-chloroquinoline-3-carboxylate (**6**)

To a suspension of **5** (4.00 g, 13.6 mmol) in POCl_3 (15.0 mL) was added catalytic amount of *N,N*-dimethylformamide (DMF) and the mixture was heated to reflux for 4 h. It was then cooled to room temperature and carefully poured onto ice. After vigorous agitation, the precipitate was filtered, washed with water and dissolved in DCM. The solution was subsequently washed with saturated NaHCO_3 solution, brine, dried with anhydrous Na_2SO_4 and concentrated in vacuo to provide the title intermediate as a light yellow solid. Yield: 93%; ^1H NMR (500 MHz, CDCl_3): δ 9.21 (s, 1H, Ar-H), 8.47 (d, 1.5 Hz, 1H, Ar-H), 8.02 (d, 9.0 Hz, 1H, Ar-H), 7.95 (dd, 1.5 Hz, 9.0 Hz, 1H, Ar-H), 4.40 (q, 7.0 Hz, 2H, CH_2), 1.60 (t, 7.0 Hz, 3H, CH_3). ESI-MS: $m/z = 314$ $[\text{M}+\text{H}]^+$.

4.1.4. General procedure for the preparation of intermediates **7a** and **7b** (A)

To a solution of **6** (1.0 equiv) in acetic acid (2 mL/1 mmol substrate) AcONa (1.4 equiv) and substituted aniline (1.0 equiv), such as **2** or 3-trifluoromethylaniline, were added. The resultant mixture was stirred for 0.5 h at room temperature and quenched with water. After the crude product was totally precipitated, it was filtered, washed with water and dissolved in DCM. The solution was then washed with saturated NaHCO_3 solution, brine and dried over anhydrous Na_2SO_4 . Following removal of solvent in vacuo, the residue was purified via flash column chromatography using EA/PE (1:6) as eluent to afford corresponding ethyl 6-bromo-4-anilino-3-carboxylate quinoline derivative **7a** or **7b** as light yellow solid.

4.1.4.1. Ethyl 6-bromo-4-((4-(2-cyanopropan-2-yl)phenyl)amino)quinoline-3-carboxylate (7a**).** Light yellow solid; yield: 83%; ESI-MS: $m/z = 438$ $[\text{M}+\text{H}]^+$.

4.1.4.2. Ethyl 6-bromo-4-((3-(trifluoromethyl)phenyl)amino)quinoline-3-carboxylate (7b**).** Light yellow solid; yield: 91%; ^1H NMR (500 MHz, $\text{DMSO}-d_6$): δ 9.70 (s, 1H, NH), 8.78 (s, 1H, Ar-H), 8.52 (d, 1.5 Hz, 1H, Ar-H), 7.95 (dd, 1.5 Hz, 9.0 Hz, 1H, Ar-H), 7.92 (d, 9.0 Hz, 1H, Ar-H), 7.49 (t, 8.5 Hz, 1H, Ar-H), 7.33

(s, 1H, Ar-H), 7.32 (d, 2.0 Hz, 1H, Ar-H), 7.27 (dd, 2.0 Hz, 8.5 Hz, 1H, Ar-H), 3.81 (q, 7.0 Hz, 2H, CH₂), 1.01 (t, 7.0 Hz, 3H, CH₃). ESI-MS: *m/z* = 439 [M+H]⁺.

4.1.5. General procedure for the preparation of intermediates 8a–c (B)

A mixture containing **7a** or **7b** and the concentrated solution of NH₃ in EtOH (4 mL/1 mmol substrate) in a sealed tube was heated at 80 °C for 8 h. It was then cooled to –20 °C and filtered to collect the filtrate. After removal of the solvent, the residue was purified via flash column chromatography using EA/PE/TEA (30:10:1) as the eluent to afford corresponding 6-bromo-4-(phenylamino)quinoline-3-carboxamide derivative **8a** or **8c** as light yellow solid.

The intermediate **8b** was prepared by treatment of **7a** with the concentrated solution of MeNH₂ in EtOH (2 mL/1 mmol substrate) in a sealed tube at 80 °C for 2 h. The mixture was then cooled and the solvent was removed in vacuo. The resultant residue was purified via flash column chromatography using EA/PE/TEA (60:40:1–60:20:1) as eluent to afford the desired intermediate as light yellow solid.

4.1.5.1. 6-Bromo-4-((4-(2-cyanopropan-2-yl)phenyl)amino)quinoline-3-carboxamide (8a). Light yellow solid; yield: 46%; ¹H NMR (500 MHz, DMSO-*d*₆): δ 10.21 (s, 1H, NH), 8.94 (s, 1H, Ar-H), 8.16 (br s, 1H, NH), 8.00 (d, 2.0 Hz, 1H, Ar-H), 7.88 (d, 9.0 Hz, 1H, Ar-H), 7.82 (dd, 2.0 Hz, 9.0 Hz, 1H, Ar-H), 7.65 (br s, 1H, NH), 7.39 (d, 9.0 Hz, 2H, Ar-H), 7.01 (d, 9.0 Hz, 2H, Ar-H), 1.65 (s, 6H, CH₃×2). ESI-MS: *m/z* = 409 [M+H]⁺.

4.1.5.2. 6-Bromo-4-((4-(2-cyanopropan-2-yl)phenyl)amino)-*N*-methylquinoline-3-carboxamide (8b). Light yellow solid; yield: 89%; ¹H NMR (500 MHz, DMSO-*d*₆): δ 9.63 (s, 1H, NH); 8.72 (s, 1H, Ar-H), 8.36 (q, 4.5 Hz, 1H, NH), 8.31 (d, 2.0 Hz, 1H, Ar-H), 7.87 (d, 9.0 Hz, 1H, Ar-H), 7.84 (dd, 2.0 Hz, 9.0 Hz, 1H, Ar-H), 7.36 (d, 9.0 Hz, 2H, Ar-H), 7.00 (d, 9.0 Hz, 2H, Ar-H), 2.42 (d, 4.5 Hz, 3H, Ar-H), 1.65 (s, 6H, CH₃×2). ESI-MS: *m/z* = 423 [M+H]⁺.

4.1.5.3. 6-Bromo-4-((3-(trifluoromethyl)phenyl)amino)quinoline-3-carboxamide (8c). Light yellow solid; yield: 52%; ¹H NMR (500 MHz, CDCl₃): δ 10.94 (s, 1H, NH), 9.53 (br s, 1H, NH), 9.01 (s, 1H, Ar-H), 7.93 (d, 9.0 Hz, 1H, Ar-H), 7.79–7.71 (m, 2H, Ar-H), 7.45–7.38 (m, 2H, Ar-H), 7.27 (s, 1H, Ar-H), 7.16 (d, 7.5 Hz, 1H, Ar-H). ESI-MS: *m/z* = 410 [M+H]⁺.

4.1.6. General procedure for the preparation of target compounds 9a–h (C)

To a solution of the intermediate **8a** (or **8b**, **8c**) (1.0 equiv) in H₂O/1,4-dioxane (1:3, V/V) were added anhydrous potassium carbonate (1.1 equiv), corresponding borate (1.1 equiv), such as 1-methyl-1*H*-pyrazole-5-boronic acid pinacol ester, quinoline-3-boronic acid pinacol ester, 2-aminopyridine-5-boronic acid pinacol ester, or 2-methoxypyridine-5-boronic acid pinacol ester, and Pd (Ph₃P)₄ (0.08 equiv). The resultant suspension was stirred at 100 °C for 8 h under N₂ atmosphere. After this time, the reaction mixture was cooled and concentrated in vacuo. The residue was treated with EtOAc, and following filtration, the filtrate was washed with water and brine. Afterwards, the organic layer was dried over anhydrous Na₂SO₄ and evaporated in vacuo. The residue was subjected to flash column chromatography using EA/MeOH/TEA (160:3:2) as eluent, which afforded compounds **9a–h** as light yellow solid.

4.1.6.1. 4-((4-(2-Cyanopropan-2-yl)phenyl)amino)-6-(1-methyl-1*H*-pyrazol-5-yl)quinoline-3-carboxamide (9a). Light yellow solid; yield: 73%; ¹H NMR (500 MHz, DMSO-*d*₆): 10.63 (s, 1H, NH), 9.04 (s, 1H, Ar-H), 8.33 (br s, 1H, NH), 8.01 (d, 9.0 Hz, 1H,

Ar-H), 7.85 (dd, 2.0 Hz, 9.0 Hz, 1H, Ar-H), 7.79 (d, 2.0 Hz, 1H, Ar-H), 7.76 (br s, 1H, NH), 7.43 (d, 8.5 Hz, 2H, Ar-H), 7.40 (d, 1.5 Hz, 1H, Ar-H), 7.08 (d, 8.5 Hz, 2H, Ar-H), 6.22 (d, 1.5 Hz, 1H, Ar-H), 3.48 (s, 3H, Pyrazole *N*-CH₃), 1.66 (s, 6H, CH₃×2); ESI-MS: *m/z* = 411 [M+H]⁺; mp 258–260 °C; HPLC: *t*_R = 12.29 min, flow rate 0.8 mL/min, COSMOSIL 5C18-MS-II column (4.6ID × 250 mm), rt, eluent A-80%, eluent B-20%.

4.1.6.2. 4'-((4-(2-Cyanopropan-2-yl)phenyl)amino)-[3,6'-biquinoline]-3'-carboxamide (9b). Light yellow solid; yield: 65%; ¹H NMR (500 MHz, DMSO-*d*₆): 10.64 (br s, 1H, NH), 9.00 (s, 1H, Ar-H), 8.83 (d, 2.5 Hz, 1H, NH), 8.47 (d, 2.5 Hz, 1H, NH), 8.23 (dd, 1.5 Hz, 8.5 Hz, 2H, Ar-H), 8.19 (d, 1.5 Hz, 1H, Ar-H), 8.08 (d, 8.5 Hz, 1H, Ar-H), 8.01 (d, 7.5 Hz, 1H, Ar-H), 7.97 (d, 7.5 Hz, 1H, Ar-H), 7.78–7.75 (m, 1H, Ar-H), 7.69 (s, 1H, Ar-H), 7.65–7.62 (m, 1H, Ar-H), 7.49 (d, 8.5 Hz, 2H, Ar-H), 7.15 (d, 8.5 Hz, 2H, Ar-H), 1.70 (s, 6H, CH₃×2); ¹³C NMR (125 MHz, DMSO-*d*₆): δ 170.03, 150.64, 149.56, 149.50, 149.01, 147.27, 143.16, 136.96, 133.63, 133.51, 132.37, 130.76, 130.28, 130.01, 129.19, 128.75, 127.86, 127.67, 126.56, 125.20, 124.06, 121.73, 120.79, 113.48, 36.77, 28.95; ESI-MS: *m/z* = 458 [M+H]⁺; mp 200–203 °C; HPLC: *t*_R = 7.28 min, flow rate 1.0 mL/min, Diamonsil™ C18 5μ 4.6 × 200 mm, rt, eluent A-50%, eluent B-50%.

4.1.6.3. 4'-((4-(2-Cyanopropan-2-yl)phenyl)amino)-*N*-methyl-[3,6'-biquinoline]-3'-carboxamide (9c). Light yellow solid; yield: 82%; ¹H NMR (500 MHz, DMSO-*d*₆): 9.94 (s, 1H, NH), 9.10 (d, 2.0 Hz, 1H, Ar-H), 8.78 (s, 1H, Ar-H), 8.61 (d, 2.0 Hz, 1H, Ar-H), 8.49 (d, 2.0 Hz, 1H, Ar-H), 8.44 (q, 4.5 Hz, 1H, NH), 8.26 (dd, 2.0 Hz, 9.0 Hz, 1H, Ar-H), 8.08 (d, 9.0 Hz, 1H, Ar-H), 8.05–8.00 (m, 2H, Ar-H), 7.79–7.75 (m, 1H, Ar-H), 7.67–7.62 (m, 1H, Ar-H), 7.44 (d, 9.0 Hz, 2H, Ar-H), 7.10 (d, 9.0 Hz, 2H, Ar-H), 2.52 (d, 4.5 Hz, 3H, *N*-CH₃), 1.68 (s, 6H, CH₃×2); ¹³C NMR (125 MHz, DMSO-*d*₆): δ 167.78, 150.73, 149.84, 149.34, 147.34, 147.12, 142.83, 136.51, 134.03, 133.56, 132.52, 130.84, 130.23, 129.73, 129.21, 128.80, 127.96, 127.65, 126.18, 125.22, 123.22, 121.35, 121.32, 114.98, 36.73, 28.95, 26.31; ESI-MS: *m/z* = 472 [M+H]⁺; mp 248–250 °C; HPLC: *t*_R = 7.63 min, flow rate 1.0 mL/min, Diamonsil™ C18 5μ 4.6 × 200 mm, rt, eluent A-50%, eluent B-50%.

4.1.6.4. 6-(6-Aminopyridin-3-yl)-4-((4-(2-cyanopropan-2-yl)phenyl)amino)quinoline-3-carboxamide (9d). Light yellow solid; yield: 79%; ¹H NMR (500 MHz, DMSO-*d*₆): δ 10.68 (s, 1H, NH), 8.97 (s, 1H, Ar-H), 8.31 (s, 1H, Ar-H), 7.99–7.90 (m, 3H, Ar-H), 7.76 (s, 2H, NH×2), 7.48 (d, 8.5 Hz, 2H, Ar-H), 7.31 (dd, 2.0 Hz, 8.5 Hz, 1H, Ar-H), 7.11 (d, 8.5 Hz, 2H, Ar-H), 6.43 (d, 8.5 Hz, 1H, Ar-H), 6.18 (s, 2H, NH×2), 1.72 (s, 6H, CH₃×2); ¹³C NMR (125 MHz, DMSO-*d*₆): δ 170.31, 159.83, 149.66, 148.94, 148.79, 146.59, 143.33, 136.73, 135.62, 134.78, 130.52, 129.05, 126.49, 125.20, 123.33, 121.72, 121.38, 120.65, 113.09, 108.35, 36.75, 28.95; ESI-MS: *m/z* = 423 [M+H]⁺; mp 266–267 °C; HPLC: *t*_R = 9.17 min, flow rate 0.8 mL/min, COSMOSIL 5C18-MS-II column (4.6ID × 250 mm), rt, eluent A-80%, eluent B-20%.

4.1.6.5. 6-(6-Aminopyridin-3-yl)-4-((4-(2-cyanopropan-2-yl)phenyl)amino)-*N*-methylquinoline-3-carboxamide (9e). Light yellow solid; yield: 70%; ¹H NMR (500 MHz, DMSO-*d*₆): 9.98 (s, 1H, NH), 8.74 (s, 1H, Ar-H), 8.50 (q, 4.5 Hz, 1H, NH), 8.10 (d, 2.0 Hz, 1H, Ar-H), 8.02–7.88 (m, 3H, Ar-H), 7.48 (dd, 2.0 Hz, 8.5 Hz, 1H, Ar-H), 7.42 (d, 9.0 Hz, 2H, Ar-H), 7.04 (d, 9.0 Hz, 2H, Ar-H), 6.46 (d, 8.5 Hz, 1H, Ar-H), 6.12 (s, 2H, NH), 2.56 (d, 4.5 Hz, 3H, *N*-CH₃), 1.68 (s, 6H, CH₃×2); ¹³C NMR (125 MHz, DMSO-*d*₆): δ 167.52, 159.36, 149.01, 148.09, 146.50, 146.19, 142.54, 135.80, 135.26, 134.67, 129.93, 128.34, 125.68, 124.72, 122.94, 120.73, 120.69, 120.01, 114.11, 107.87, 36.20, 28.44, 25.88; ESI-MS: *m/z* = 437 [M+H]⁺; mp 215–218 °C; HPLC:

$t_R = 7.23$ min, flow rate 0.9 mL/min, COSMOSIL 5C18-MS-II column (4.6ID \times 250 mm), rt, eluent A-75%, eluent B-25%.

4.1.6.6. 4-((4-(2-Cyanopropan-2-yl)phenyl)amino)-6-(6-methoxy-pyridin-3-yl)quinoline-3-carboxamide (9f). Light yellow solid; yield: 74%; $^1\text{H NMR}$ (500 MHz, DMSO- d_6): 10.73 (s, 1H, NH), 8.99 (s, 1H, Ar-H), 8.30 (br s, 1H, NH), 8.11 (d, 2.5 Hz, 1H, Ar-H), 8.03 (dd, 1.5 Hz, 8.5 Hz, 1H, Ar-H), 8.00 (d, 8.5 Hz, 1H, Ar-H), 7.86 (d, 1.5 Hz, 1H, Ar-H), 7.73 (br s, 1H, NH), 7.71 (dd, 2.5 Hz, 8.5 Hz, 1H, Ar-H), 7.50 (d, 8.5 Hz, 2H, Ar-H), 7.14 (d, 8.5 Hz, 2H, Ar-H), 6.84 (d, 8.5 Hz, 1H, Ar-H), 3.86 (s, 3H, OCH₃), 1.73 (s, 6H, CH₃ \times 2); $^{13}\text{C NMR}$ (125 MHz, DMSO- d_6): δ 169.75, 163.12, 149.80, 148.88, 148.55, 144.85, 142.68, 137.24, 136.58, 132.91, 130.18, 128.92, 128.40, 126.12, 124.73, 122.48, 121.57, 119.95, 112.34, 110.57, 53.21, 36.23, 28.34; ESI-MS: $m/z = 438$ [M+H] $^+$; mp 250–252 $^\circ\text{C}$; HPLC: $t_R = 8.15$ min, flow rate 1.0 mL/min, DiamonsilTM C18 5 μ 4.6 \times 200 mm, rt, eluent A-60%, eluent B-40%.

4.1.6.7. 6-(6-Aminopyridin-3-yl)-4-((3-(trifluoromethyl)phenyl)amino)quinoline-3-carboxamide (9g). Light yellow solid; yield: 67%; $^1\text{H NMR}$ (500 MHz, DMSO- d_6): 10.12 (s, 1H, NH), 8.89 (s, 1H, Ar-H), 8.18–8.10 (m, 2H, Ar-H), 8.09–7.96 (m, 3H, Ar-H, NH), 7.64 (br s, 1H, NH), 7.63 (s, 1H, Ar-H), 7.48 (t, 8.0 Hz, 1H, Ar-H), 7.37–7.30 (m, 2H), 7.25 (d, 8.0 Hz, 1H, Ar-H), 6.50 (d, 8.0 Hz, 1H, Ar-H), 6.20 (s, 2H, NH); $^{13}\text{C NMR}$ (125 MHz, DMSO- d_6): δ 169.45, 159.91, 149.97, 148.69, 148.64, 146.58, 146.21, 144.80, 135.83, 135.67, 130.55, 130.27 ($J_{\text{C-F}}$ 31.25 Hz), 129.20, 124.57 ($J_{\text{C-F}}$ 271.25 Hz), 123.39, 123.17, 121.69, 120.22, 118.68 ($J_{\text{C-F}}$ 2.50 Hz), 116.03, 115.91 ($J_{\text{C-F}}$ 2.50 Hz), 108.42; ESI-MS: $m/z = 424$ [M+H] $^+$; mp 275–277 $^\circ\text{C}$; HPLC: $t_R = 7.32$ min, flow rate 0.9 mL/min, COSMOSIL 5C18-MS-II column (4.6ID \times 250 mm), rt, eluent A-75%, eluent B-25%.

4.1.6.8. 4'-((3-(Trifluoromethyl)phenyl)amino)-[3,6'-biquinoline]-3'-carboxamide (9h). Light yellow solid; yield: 76%; $^1\text{H NMR}$ (500 MHz, CDCl₃): 12.62 (br s, 1H, NH), 9.75 (s, 1H, Ar-H), 8.74 (s, 1H, Ar-H), 8.51 (d, 8.5 Hz, 1H, Ar-H), 8.15 (d, 9.0 Hz, 1H, Ar-H), 8.12 (d, 9.0 Hz, 1H, Ar-H), 7.86 (s, 1H, Ar-H), 7.84 (s, 1H, Ar-H), 7.76–7.72 (m, 2H, Ar-H), 7.71 (d, 8.5 Hz, 1H, Ar-H), 7.66–7.62 (m, 1H, Ar-H), 7.60–7.58 (m, 1H, Ar-H), 7.56 (s, 1H, Ar-H), 7.47 (d, 8.5 Hz, 1H, Ar-H); $^{13}\text{C NMR}$ (125 MHz, DMSO- d_6): δ 168.73, 150.68, 149.29, 149.01, 148.97, 146.85, 145.87, 144.11, 133.94, 133.21, 131.97, 130.48, 130.12, 129.85, 129.79 ($J_{\text{C-F}}$ 32.50 Hz), 129.60, 128.69, 128.28, 127.47, 127.27, 123.82 ($J_{\text{C-F}}$ 275.00 Hz), 122.85, 122.62, 121.19, 118.46 ($J_{\text{C-F}}$ 3.75 Hz), 115.62; ESI-MS: $m/z = 459$ [M+H] $^+$; mp 212–215 $^\circ\text{C}$; HPLC: $t_R = 10.36$ min, flow rate 1.0 mL/min, DiamonsilTM C18 5 μ 4.6 \times 200 mm, rt, eluent A-60%, eluent B-40%.

4.1.7. *tert*-Butyl 4-(4-amino-2-(trifluoromethyl)phenyl)piperazine-1-carboxylate (11)

To a suspension of anhydrous potassium carbonate (7.30 g, 53.0 mmol, 1.2 equiv) and 1-chloro-4-nitro-2-(trifluoromethyl)benzene **10** (10.0 g, 44.3 mmol, 1.0 equiv) in DMF (25 mL) was added *N*-Boc-piperazine (8.23 g, 44.3 mmol, 1.0 equiv) at room temperature. The resultant mixture was stirred at 40 $^\circ\text{C}$ for 12 h and then evaporated in vacuo to remove the solvent. Afterwards, the residue was treated with EtOAc and water. The organic layer was washed with brine, and dried over anhydrous Na₂SO₄. Following removal of EtOAc in vacuo, the residue slowly solidified to give *tert*-butyl 4-(4-nitro-2-(trifluoromethyl)phenyl)piperazine-1-carboxylate as light yellow solid. Yield: 92%, ESI-MS: $m/z = 376$ [M+H] $^+$. The resultant product (6.11 g, 16.3 mmol) and 10% Pd/C (10% of the substrate, w/w) were shacked in methanol (100 mL) and the suspension was stirred at room temperature under H₂ (balloon) atmosphere overnight. After this time, Pd/C was filtered and

the filtrate was concentrated in vacuo to provide the **11** as a white solid after recrystallization from EtOH. Yield: 87%. ESI-MS: $m/z = 346$ [M+H] $^+$; mp 140–141 $^\circ\text{C}$.

4.1.8. Ethyl 6-bromo-4-((4-(4-(*tert*-butoxycarbonyl)piperazin-1-yl)-3-(trifluoromethyl)phenyl)amino)quinoline-3-carboxylate (12)

The preparation of **12** is according to general procedure A via the SNAr reaction between **6** and **11** in the presence of AcONa.

Light yellow solid; yield: 89%; $^1\text{H NMR}$ (500 MHz, DMSO- d_6): 9.68 (s, 1H, NH), 8.84 (s, 1H, Ar-H), 8.54 (d, 2.0 Hz, 1H, Ar-H), 7.95 (dd, 2.0 Hz, 9.0 Hz, 1H, Ar-H), 7.92 (d, 9.0 Hz, 1H, Ar-H), 7.53 (d, 8.5 Hz, 1H, Ar-H), 7.35 (d, 2.5 Hz, 1H, Ar-H), 7.27 (dd, 2.5 Hz, 8.5 Hz, 1H, Ar-H), 3.82 (q, 2.0 Hz, 2H, CH₂), 3.51–3.37 (m, 4H, Piperazine-CH₂ \times 2), 2.77 (t, 4.5 Hz, 4H, Piperazine-CH₂ \times 2), 1.43 (s, 9H, Boc-CH₃ \times 3), 1.01 (t, 2.0 Hz, 3H, CH₃); ESI-MS: $m/z = 623$ [M+H] $^+$.

4.1.9. General procedure for the preparation of intermediates 13a–c

The synthetic procedure of intermediates **13a–c** is similar to general procedure B, except for the intermediate **13c**. It was prepared by treatment of **12** with cyclopropylamine (1 mL/100 mg substrate) in the sealed tube at 80 $^\circ\text{C}$ for 24 h. Afterwards, the excessive cyclopropylamine was removed in vacuo and the residue was purified via flash column chromatography using EA/PE/TEA (60:40:1–60:20:1) as eluent to afford **13c** as light yellow solid.

4.1.9.1. *tert*-Butyl 4-(4-((6-bromo-3-carbamoylquinolin-4-yl)amino)-2-(trifluoromethyl)phenyl)piperazine-1-carboxylate (13a).

Light yellow solid; yield: 53%; $^1\text{H NMR}$ (500 MHz, DMSO- d_6): 9.91 (s, 1H, NH), 8.90 (s, 1H, Ar-H), 8.21 (d, 2.0 Hz, 1H, Ar-H), 8.08 (br s, 1H, NH), 7.92 (d, 9.0 Hz, 1H, Ar-H), 7.89 (dd, 2.0 Hz, 9.0 Hz, 1H, Ar-H), 7.61 (br s, 1H, NH), 7.46 (d, 8.5 Hz, 1H, Ar-H), 7.29 (d, 3.0 Hz, 1H, Ar-H), 7.18 (dd, 3.0 Hz, 8.5 Hz, 1H, Ar-H), 3.49–3.36 (m, 4H, Piperazine-CH₂ \times 2), 2.77 (t, 4.5 Hz, 4H, Piperazine-CH₂ \times 2), 1.43 (s, 9H, Boc-CH₃ \times 3); ESI-MS: $m/z = 594$ [M+H] $^+$.

4.1.9.2. *tert*-Butyl 4-(4-((6-bromo-3-(methylcarbamoyl)quinolin-4-yl)amino)-2-(trifluoromethyl)phenyl)piperazine-1-carboxylate (13b).

Light yellow solid; yield: 86%; $^1\text{H NMR}$ (500 MHz, DMSO- d_6): 9.48 (s, 1H, NH), 8.66 (s, 1H, Ar-H), 8.52 (s, 1H, Ar-H), 8.38 (q, 4.5 Hz, NH), 7.90 (d, 1.0 Hz, 2H, Ar-H), 7.46 (d, 8.5 Hz, 1H, Ar-H), 7.25 (d, 2.5 Hz, 1H, Ar-H), 7.18 (dd, 2.5 Hz, 8.5 Hz, 1H, Ar-H), 3.49–3.39 (m, 4H, Piperazine-CH₂ \times 2), 2.77 (t, 4.5 Hz, 4H, Piperazine-CH₂ \times 2), 2.35 (d, 4.5 Hz, 3H, N-CH₃), 1.43 (s, 9H, Boc-CH₃ \times 3); ESI-MS: $m/z = 608$ [M+H] $^+$.

4.1.9.3. *tert*-Butyl 4-(4-((6-bromo-3-(cyclopropylcarbamoyl)quinolin-4-yl)amino)-2-(trifluoromethyl)phenyl)piperazine-1-carboxylate (13c).

Light yellow solid; yield: 57%; $^1\text{H NMR}$ (500 MHz, DMSO- d_6): 9.33 (s, 1H, NH), 8.66 (s, 1H, Ar-H), 8.59 (t, 1.0 Hz, 1H, Ar-H), 8.43 (d, 3.5 Hz, 1H, NH), 7.91 (d, 1.0 Hz, 2H, Ar-H), 7.46 (d, 8.5 Hz, 1H, Ar-H), 7.23 (d, 2.5 Hz, 1H, Ar-H), 7.13 (dd, 2.5 Hz, 8.5 Hz, 1H, Ar-H), 3.49–3.38 (m, 4H, Piperazine-CH₂ \times 2), 2.77 (t, 4.5 Hz, 4H, Piperazine-CH₂ \times 2), 2.36–2.27 (m, 1H, N-CH), 1.43 (s, 9H, Boc-CH₃ \times 3), 0.60–0.54 (m, 2H, CH \times 2), 0.48–0.42 (m, 2H, CH \times 2); ESI-MS: $m/z = 634$ [M+H] $^+$.

4.1.10. General procedure for the preparation of intermediates 14a–e

The synthetic procedure of intermediates **14a–e** is according to general procedure C.

4.1.10.1. *tert*-Butyl 4-(4-((3'-carbamoyl-[3,6'-biquinolin]-4'-yl)amino)-2-(trifluoromethyl)phenyl)piperazine-1-carboxylate (14a).

Light yellow solid; yield: 72%; $^1\text{H NMR}$ (500 MHz,

DMSO- d_6): 10.28 (s, 1H, NH), 9.07 (d, 2.5 Hz, 1H, Ar-H), 8.95 (s, 1H, Ar-H), 8.59 (d, 1.5 Hz, 1H, Ar-H), 8.35 (d, 1.0 Hz, 1H, Ar-H), 8.29 (dd, 1.5 Hz, 8.5 Hz, 1H, Ar-H), 8.17 (br s, 1H, NH), 8.13 (d, 8.5 Hz, 1H, Ar-H), 8.06 (d, 8.0 Hz, 1H, Ar-H), 8.02 (d, 8.5 Hz, 1H, Ar-H), 7.83–7.77 (m, 1H, Ar-H), 7.70–7.66 (m, 1H, Ar-H), 7.65 (br s, 1H, NH), 7.52 (d, 8.5 Hz, 1H, Ar-H), 7.41 (d, 2.5 Hz, 1H, Ar-H), 7.29 (dd, 2.5 Hz, 8.5 Hz, 1H, Ar-H), 3.48–3.38 (m, 4H, Piperazine-CH₂×2), 2.79 (t, 4.5 Hz, 4H, Piperazine-CH₂×2), 1.43 (s, 9H, Boc-CH₃×3); ESI-MS: m/z = 643 [M+H]⁺.

4.1.10.2. tert-Butyl 4-(4-((3'-(methylcarbamoyl)-[3,6'-biquinolin]-4'-yl)amino)-2-(trifluoromethyl)phenyl)piperazine-1-carboxylate (14b). Light yellow solid; yield: 79%; ¹H NMR (500 MHz, DMSO- d_6): 9.70 (s, 1H, NH), 9.34 (d, 2.0 Hz, 1H, Ar-H), 8.76 (d, 2.0 Hz, 1H, Ar-H), 8.72 (s, 1H, Ar-H), 8.70 (s, 1H, Ar-H), 8.43 (q, 4.5 Hz, 1H, Ar-H), 8.32 (dd, 1.5 Hz, 8.5 Hz, 1H, Ar-H), 8.12 (d, 8.5 Hz, 1H, Ar-H), 8.10–8.04 (m, 2H, Ar-H), 7.84–7.77 (m, 1H, Ar-H), 7.72–7.66 (m, 1H, Ar-H), 7.51 (d, 8.5 Hz, 1H, Ar-H), 7.34 (d, 2.5 Hz, 1H, Ar-H), 7.27 (dd, 2.5 Hz, 8.5 Hz, 1H, Ar-H), 3.51–3.38 (m, 4H, Piperazine-CH₂×2), 2.79 (t, 4.5 Hz, 4H, Piperazine-CH₂×2), 2.40 (d, 4.5 Hz, 3H, CH₃), 1.43 (s, 9H, Boc-CH₃×3); ESI-MS: m/z = 657 [M+H]⁺.

4.1.10.3. tert-Butyl 4-(4-((3'-(cyclopropylcarbamoyl)-[3,6'-biquinolin]-4'-yl)amino)-2-(trifluoromethyl)phenyl)piperazine-1-carboxylate (14c). Light yellow solid; yield: 65%; ¹H NMR (500 MHz, DMSO- d_6): 9.51 (s, 1H, NH), 9.39 (d, 2.0 Hz, 1H, Ar-H), 8.79 (d, 2.0 Hz, 1H, Ar-H), 8.78 (d, 2.5 Hz, 1H, Ar-H), 8.71 (s, 1H, Ar-H), 8.46 (d, 3.5 Hz, 1H, NH), 8.33 (dd, 2.0 Hz, 8.5 Hz, 1H, Ar-H), 8.13 (d, 8.5 Hz, 1H, Ar-H), 8.10–8.07 (m, 2H, Ar-H), 7.84–7.78 (m, 1H, Ar-H), 7.72–7.66 (m, 1H, Ar-H), 7.50 (d, 8.5 Hz, 1H, Ar-H), 7.32 (d, 2.5 Hz, 1H, Ar-H), 7.22 (dd, 2.5 Hz, 8.5 Hz, 1H, Ar-H), 3.49–3.39 (m, 4H, Piperazine-CH₂×2), 2.79 (t, 4.5 Hz, 4H, Piperazine-CH₂×2), 2.42–2.35 (m, 1H, N-CH), 1.44 (s, 9H, Boc-CH₃×3), 0.52–0.43 (m, 2H, CH×2), 0.12–0.05 (m, 2H, CH×2); ESI-MS: m/z = 683 [M+H]⁺.

4.1.10.4. tert-Butyl 4-(4-((3-carbamoyl-6-(6-methoxyppyridin-3-yl)quinolin-4-yl)amino)-2-(trifluoromethyl)phenyl)piperazine-1-carboxylate (14d). Light yellow solid; yield: 81%; ¹H NMR (500 MHz, DMSO- d_6): 10.35 (s, 1H, NH), 8.94 (s, 1H, Ar-H), 8.23 (d, 2.0 Hz, 1H, Ar-H), 8.19 (br s, 1H, NH), 8.06 (dd, 2.0 Hz, 8.5 Hz, 1H, Ar-H), 8.04 (s, 1H, Ar-H), 8.02–8.00 (m, 1H, Ar-H), 7.89 (dd, 2.5 Hz, 8.5 Hz, 1H, Ar-H), 7.67 (br s, 1H, NH), 7.54 (d, 8.5 Hz, 1H, Ar-H), 7.36 (d, 2.5 Hz, 1H, Ar-H), 7.28 (dd, 2.5 Hz, 8.5 Hz, 1H, Ar-H), 6.90 (d, 8.5 Hz, 1H, Ar-H), 3.89 (s, 3H, OCH₃), 3.49–3.39 (m, 4H, Piperazine-CH₂×2), 2.82 (t, 4.5 Hz, 4H, Piperazine-CH₂×2), 1.43 (s, 9H, Boc-CH₃×3); ESI-MS: m/z = 623 [M+H]⁺.

4.1.10.5. tert-Butyl 4-(4-((3-carbamoyl-6-(1-methyl-1H-pyrazol-5-yl)quinolin-4-yl)amino)-2-(trifluoromethyl)phenyl)piperazine-1-carboxylate (14e). Light yellow solid; yield: 74%; ¹H NMR (500 MHz, DMSO- d_6): 10.33 (s, 1H, NH), 9.02 (s, 1H, Ar-H), 8.27 (br s, 1H, NH), 8.07 (d, 8.5 Hz, 1H, Ar-H), 7.93 (d, 1.5 Hz, 1H, Ar-H), 7.90 (dd, 1.5 Hz, 8.5 Hz, 1H, Ar-H), 7.73 (br s, 1H, NH), 7.49 (d, 8.5 Hz, 1H, Ar-H), 7.47 (d, 2.0 Hz, 1H, Ar-H), 7.34 (d, 2.5 Hz, 1H, Ar-H), 7.22 (dd, 2.5 Hz, 8.5 Hz, 1H, Ar-H), 6.31 (d, 2.0 Hz, 1H, Ar-H), 3.60 (s, 3H, Pyrazole N-CH₃), 3.50–3.38 (m, 4H, Piperazine-CH₂×2), 2.77 (t, 4.5 Hz, 4H, Piperazine-CH₂×2), 1.43 (s, 9H, Boc-CH₃×3); ESI-MS: m/z = 596 [M+H]⁺.

4.1.11. General procedure for the preparation of target compounds 15a–d or the intermediate 15e (D)

To a solution of intermediate **14a** (or **14b–e**) in EtOAc (20 mL/1 mmol substrate) was added EtOAc, saturated with hydrogen chloride (10 mL/1 mmol substrate), dropwise at 0 °C. During

this process, a little hydrochloride of the Boc-protected product was precipitated and the suspension was stirred at the room temperature for 3 h. After removal of solvent, the resultant solid was washed with diethyl ether and dried in vacuo to afford target compound **15a** (or **15b–d**) or the intermediate **15e**.

4.1.11.1. Hydrochloride of 4-((4-(piperazin-1-yl)-3-(trifluoromethyl)phenyl)amino)-[3,6'-biquinoline]-3'-carboxamide (15a). Yellow solid; yield: 97%; ¹H NMR (500 MHz, DMSO- d_6): 12.11 (s, 1H, HCl), 9.45 (s, 1H, Piperazine-NH), 9.31 (s, 2H, NH, Ar-H), 9.15 (s, 1H, Ar-H), 9.10 (s, 1H, Ar-H), 8.98 (s, 1H, Ar-H), 8.64 (d, 9.0 Hz, 1H, Ar-H), 8.30 (d, 9.0 Hz, 1H, Ar-H), 8.28 (br s, 1H, NH), 8.18 (d, 8.0 Hz, 1H, Ar-H), 8.15 (d, 8.0 Hz, 1H, Ar-H), 7.94–7.91 (m, 1H, Ar-H), 7.81–7.78 (m, 1H, Ar-H), 7.74 (s, 1H, Ar-H), 7.72–7.68 (m, 2H, Ar-H, NH), 7.60 (d, 8.5 Hz, 1H, Ar-H), 3.25–3.17 (m, 4H, Piperazine-CH₂×2), 3.16–3.08 (m, 4H, Piperazine-CH₂×2); ESI-MS: m/z = 543 [M+H]⁺; mp 238–240 °C; HPLC: t_R = 10.96 min, flow rate 0.8 mL/min, COSMOSIL 5C18-MS-II column (4.6ID × 250 mm), rt, eluent C-60%, eluent B-40%.

4.1.11.2. Hydrochloride of N-methyl-4-((4-(piperazin-1-yl)-3-(trifluoromethyl)phenyl)amino)-[3,6'-biquinoline]-3'-carboxamide (15b). Light yellow solid; yield: 93%; ¹H NMR (500 MHz, DMSO- d_6): 12.10 (s, 1H, HCl), 10.01 (s, 1H, Piperazine-NH), 9.85 (s, 1H, NH), 9.77 (s, 1H, Ar-H), 9.60 (s, 2H, Ar-H), 8.78 (s, 1H, Ar-H), 8.69–8.64 (m, 2H, NH), 8.27 (d, 7.5 Hz, 2H, Ar-H), 8.22 (d, 7.5 Hz, 1H, Ar-H), 8.06–7.95 (m, 1H, Ar-H), 7.92–7.80 (m, 1H, Ar-H), 7.75–7.62 (m, 2H, Ar-H), 7.54 (d, 7.5 Hz, 1H, Ar-H), 3.27–2.97 (m, 8H, Piperazine-H), 2.25 (s, 3H); ¹³C NMR (125 MHz, DMSO- d_6): δ 164.02, 152.32, 148.93, 146.23, 144.39, 140.72, 140.55, 138.21, 137.17, 134.06, 133.76, 132.89, 131.62, 129.71, 129.64, 129.06, 128.44, 126.25 (J_{C-F} 27.50 Hz), 125.28, 124.14, 123.62, 123.96 (J_{C-F} 272.50 Hz), 122.54, 121.59, 120.17, 113.06, 50.28, 43.81, 25.84; ESI-MS: m/z = 557 [M+H]⁺; mp 267–270 °C; HPLC: t_R = 11.50 min, flow rate 0.8 mL/min, COSMOSIL 5C18-MS-II column (4.6ID × 250 mm), rt, eluent C-60%, eluent B-40%.

4.1.11.3. Hydrochloride of N-cyclopropyl-4-((4-(piperazin-1-yl)-3-(trifluoromethyl)phenyl)amino)-[3,6'-biquinoline]-3'-carboxamide (15c). Yellow solid; yield: 96%; ¹H NMR (500 MHz, DMSO- d_6): 11.79 (s, 1H, HCl), 9.77 (s, 1H, Piperazine-NH), 9.65 (s, 1H, NH), 9.34 (br s, 1H, NH), 9.29 (s, 2H, Ar-H), 8.81 (s, 1H, Ar-H), 8.75 (d, 3.5 Hz, 1H, Ar-H), 8.69 (d, 8.5 Hz, 1H, Ar-H), 8.30 (d, 8.5 Hz, 1H, Ar-H), 8.23–8.19 (m, 2H, Ar-H), 7.97–7.94 (m, 1H, Ar-H), 7.84–7.80 (m, 1H, Ar-H), 7.68–7.53 (m, 3H, Ar-H), 3.24–3.16 (m, 4H, Piperazine-CH₂×2), 3.15–3.04 (m, 4H, Piperazine-CH₂×2), 2.24–2.15 (m, 1H, CH), 0.53–0.46 (m, 2H, CH₂), 0.23–0.14 (m, 2H, CH₂); ¹³C NMR (125 MHz, DMSO- d_6): δ 164.54, 152.33, 148.85, 147.49, 144.78, 138.76 (J_{C-F} 6.25 Hz), 138.31, 137.60, 134.98, 133.15, 132.81, 131.62, 129.47, 129.16, 128.56, 128.41, 126.59 (J_{C-F} 27.50 Hz), 125.62, 125.52, 123.97 (J_{C-F} 271.25 Hz), 123.96, 122.40 (J_{C-F} 6.25 Hz), 121.76, 121.37, 120.43, 113.12, 50.28, 43.85, 22.89, 5.59; ESI-MS: m/z = 583 [M+H]⁺; mp 257–259 °C; HPLC: t_R = 10.00 min, flow rate 0.8 mL/min, COSMOSIL 5C18-MS-II column (4.6ID × 250 mm), rt, eluent C-50%, eluent B-50%.

4.1.11.4. Hydrochloride of 6-(6-methoxyppyridin-3-yl)-4-((4-(piperazin-1-yl)-3-(trifluoromethyl)phenyl)amino)quinoline-3-carboxamide (15d). Yellow solid; yield: 95%; ¹H NMR (500 MHz, DMSO- d_6): 12.27 (s, 1H, HCl), 9.64 (s, 2H, Piperazine-NH, NH (C-4 position of quinoline)), 8.99 (s, 1H, Ar-H), 8.70 (br s, 1H, NH), 8.43–8.35 (m, 3H, NH, Ar-H), 8.24 (d, 8.5 Hz, 1H, Ar-H), 8.15 (dd, 1.5 Hz, 8.5 Hz, 1H, Ar-H), 7.76–7.67 (m, 3H, Ar-H), 7.59 (d, 8.5 Hz, 1H, Ar-H), 6.94 (d, 8.5 Hz, 1H, Ar-H), 3.89 (s, 3H,

OCH₃), 3.27–3.09 (m, 8H, Piperazine-H); ¹³C NMR (125 MHz, DMSO-*d*₆): δ 166.95, 164.06, 153.89, 149.24, 145.65, 143.48, 138.30, 138.03, 137.84, 135.76, 132.92, 129.32, 127.68, 126.64 (*J*_{C-F} 28.75 Hz), 125.83, 123.91 (*J*_{C-F} 271.25 Hz), 123.03, 122.67, 121.59, 119.52, 111.26, 110.77, 53.95, 50.33, 43.75; ESI-MS: *m/z* = 523 [M+H]⁺; mp 266–269 °C; HPLC: *t*_R = 8.25 min, flow rate 0.8 mL/min, COSMOSIL 5C18-MS-II column (4.6ID × 250 mm), rt, eluent C-80%, eluent B-20%.

4.1.11.5. Hydrochloride of 6-(1-methyl-1H-pyrazol-5-yl)-4-((4-(piperazin-1-yl)-3-(trifluoromethyl)phenyl)amino)quinoline-3-carboxamide (15e). Light yellow solid; yield: 92%; ¹H NMR (500 MHz, DMSO-*d*₆): 12.17 (s, 1H, HCl), 9.42 (s, 2H, NH, Piperazine-NH), 9.08 (s, 1H, Ar-H), 8.48 (s, 1H, NH), 8.42 (s, 1H, NH), 8.27 (d, 8.5 Hz, 1H, Ar-H), 8.21 (dd, 1.5 Hz, 8.5 Hz, 1H, Ar-H), 7.78 (s, 1H, Ar-H), 7.72 (d, 2.0 Hz, 1H, Ar-H), 7.67 (dd, 2.0 Hz, 8.5 Hz, 1H, Ar-H), 7.58 (d, 8.5 Hz, 1H, Ar-H), 7.53 (d, 1.5 Hz, 1H, Ar-H), 6.40 (d, 1.5 Hz, 1H, Ar-H), 3.81 (s, 3H, Pyrazole N-CH₃), 3.22–3.17 (m, 4H, Piperazine-CH₂×2), 3.12–3.07 (m, 4H, Piperazine-CH₂×2); ESI-MS: *m/z* = 496 [M+H]⁺.

4.1.12. General procedure for the preparation of target compounds 16a–c (E)

Compounds **16a–c** were prepared from **15a** or **15e**. To the hydrochloride (1.0 equiv), anhydrous THF and Et₃N (3.0 equiv) were added. Subsequently, to the resultant suspension, acetyl chloride or mesyl chloride (1.2 equiv) in anhydrous THF was added dropwise at 0 °C. The reaction mixture was stirred at the same temperature for 1.5 h and concentrated in vacuo. The residue was treated with DCM and saturated NaHCO₃ solution, and the organic layer was washed with brine. Following removal of DCM in vacuo, the residue was subjected to flash column chromatography with EA/MeOH/TEA (150:3:2, for the acylated product) or EA/MeOH/TEA (300:3:3, for the mesylated product) as the eluent to give target compounds **16a–c**.

4.1.12.1. 6-(1-Methyl-1H-pyrazol-5-yl)-4-((4-(4-(methylsulfonyl)piperazin-1-yl)-3-(trifluoromethyl)phenyl)amino)quinoline-3-carboxamide (16a). Light yellow solid; yield: 72%; ¹H NMR (500 MHz, DMSO-*d*₆): 10.32 (s, 1H, NH), 9.02 (s, 1H, Ar-H), 8.26 (br s, 1H, NH), 8.07 (d, 8.5 Hz, 1H, Ar-H), 7.93 (d, 1.5 Hz, 1H, Ar-H), 7.90 (dd, 1.5 Hz, 8.5 Hz, 1H, Ar-H), 7.73 (br s, 1H, NH), 7.55 (d, 8.5 Hz, 1H, Ar-H), 7.47 (d, 1.5 Hz, 1H, Ar-H), 7.35 (d, 2.5 Hz, 1H, Ar-H), 7.24 (dd, 2.5 Hz, 8.5 Hz, 1H, Ar-H), 6.31 (d, 1.5 Hz, 1H, Ar-H), 3.61 (s, 3H, Pyrazole N-CH₃), 3.29–3.18 (m, 4H, Piperazine-CH₂×2), 2.96 (s, 3H, Methylsulfonyl), 2.91 (t, 4.5 Hz, 4H, Piperazine-CH₂×2); ¹³C NMR (125 MHz, DMSO-*d*₆): δ 168.93, 150.45, 148.83, 147.21, 145.90, 141.76, 141.15, 137.92, 130.60, 130.08, 126.77, 126.45 (*J*_{C-F} 27.50 Hz), 126.08, 124.28, 123.31 (*J*_{C-F} 283.75 Hz), 120.37, 117.97 (*J*_{C-F} 5.00 Hz), 114.87, 114.73, 106.31, 52.44, 45.97, 37.11, 33.76; ESI-MS: *m/z* = 574 [M+H]⁺; mp 246–248 °C; HPLC: *t*_R = 10.15 min, flow rate 0.9 mL/min, COSMOSIL 5C18-MS-II column (4.6ID × 250 mm), rt, eluent A-75%, eluent B-25%.

4.1.12.2. 4'-((4-(4-Acetylpiperazin-1-yl)-3-(trifluoromethyl)phenyl)amino)-[3,6'-biquinoline]-3'-carboxamide (16b). Light yellow solid; yield: 84%; ¹H NMR (500 MHz, DMSO-*d*₆): 10.29 (br s, 1H, NH), 9.06 (d, 2.0 Hz, 1H, Ar-H), 8.96 (s, 1H, Ar-H), 8.59 (d, 2.0 Hz, 1H, Ar-H), 8.36 (d, 2.0 Hz, 1H, Ar-H), 8.29 (dd, 2.0 Hz, 8.5 Hz, 1H, Ar-H), 8.17 (br s, 1H, NH), 8.13 (d, 8.5 Hz, 1H, Ar-H), 8.07 (d, 7.5 Hz, 1H, Ar-H), 8.02 (d, 7.5 Hz, 1H, Ar-H), 7.82–7.78 (m, 1H, Ar-H), 7.70–7.66 (m, 1H, Ar-H), 7.65 (br s, 1H, NH), 7.51 (d, 8.5 Hz, 1H, Ar-H), 7.41 (d, 2.5 Hz, 1H, Ar-H), 7.30 (dd, 2.5 Hz,

8.5 Hz, 1H, Ar-H), 3.60–3.49 (m, 4H, Piperazine-CH₂×2), 2.84 (t, 4.5 Hz, 2H, Piperazine-CH₂), 2.79 (t, 4.5 Hz, 2H, Piperazine-CH₂), 2.05 (s, 3H, CH₃); ¹³C NMR (125 MHz, DMSO-*d*₆): δ 169.52, 168.80, 151.05, 149.69, 149.56, 147.31, 147.26, 146.80, 141.20, 134.10, 133.56, 132.44, 130.96, 130.29, 129.97, 129.23, 128.73, 127.92, 127.71, 127.06 (*J*_{C-F} 27.50 Hz), 126.21, 124.88, 124.21 (*J*_{C-F} 271.25 Hz), 123.39, 121.21, 118.70 (*J*_{C-F} 5.00 Hz), 114.96, 53.93, 53.48, 46.75, 41.85, 21.71; ESI-MS: *m/z* = 585 [M+H]⁺; mp 261–262 °C; HPLC: *t*_R = 7.06 min, flow rate 1.0 mL/min, Diamonsil™ C18 5μ 4.6 × 200 mm, rt, eluent A-50%, eluent B-50%.

4.1.12.3. 4'-((4-(4-(Methylsulfonyl)piperazin-1-yl)-3-(trifluoromethyl)phenyl)amino)-[3,6'-biquinoline]-3'-carboxamide (16c). Light yellow solid; yield: 77%; ¹H NMR (500 MHz, DMSO-*d*₆): 10.28 (s, 1H, NH), 9.06 (d, 2.5 Hz, 1H, Ar-H), 8.96 (s, 1H, Ar-H), 8.61 (d, 2.5 Hz, 1H, Ar-H), 8.36 (d, 2.0 Hz, 1H, Ar-H), 8.29 (dd, 2.0 Hz, 8.5 Hz, 1H, Ar-H), 8.16 (br s, 1H, NH), 8.13 (d, 8.5 Hz, 1H, Ar-H), 8.07 (d, 7.5 Hz, 1H, Ar-H), 8.02 (d, 7.5 Hz, 1H, Ar-H), 7.82–7.78 (m, 1H, Ar-H), 7.70–7.66 (m, 1H, Ar-H), 7.64 (br s, 1H, NH), 7.59 (d, 8.5 Hz, 1H, Ar-H), 7.41 (d, 2.5 Hz, 1H, Ar-H), 7.32 (dd, 2.5 Hz, 8.5 Hz, 1H, Ar-H), 3.28–3.17 (m, 4H, Piperazine-CH₂×2), 3.01–2.89 (m, 7H, Piperazine-CH₂×2, Methylsulfonyl-CH₃); ¹³C NMR (125 MHz, DMSO-*d*₆): δ 169.44, 151.05, 149.72, 149.51, 147.33, 147.14, 146.48, 141.39, 134.17, 133.60, 132.45, 130.93, 130.31, 130.02, 129.24, 128.76, 127.94, 127.74, 127.08 (*J*_{C-F} 27.50 Hz), 126.45, 124.82, 124.18 (*J*_{C-F} 271.25 Hz), 123.36, 121.26, 118.59 (*J*_{C-F} 6.25 Hz), 115.10, 53.11, 46.50, 34.40; ESI-MS: *m/z* = 621 [M+H]⁺; mp 260–261 °C; HPLC: *t*_R = 8.80 min, flow rate 1.0 mL/min, Diamonsil™ C18 5μ 4.6 × 200 mm, rt, eluent A-60%, eluent B-40%.

4.1.13. Synthetic procedure for the intermediates 17 and 18

To a solution of **13a** (1.0 equiv) in DCM (10 mL/1 mmol substrate) was added TFA (TFA/DCM = 1:4, V/V) dropwise at 0 °C. The reaction mixture was then stirred at the room temperature for 6 h and concentrated in vacuo. Afterwards, the resultant oil and anhydrous Et₃N (3.0 equiv) were dissolved in anhydrous THF (10 mL/1 mmol substrate). To the solution, propionyl chloride (1.2 equiv) in anhydrous THF (5 mL/1 mmol substrate) was added dropwise at 0 °C. The reaction mixture was stirred at the same temperature for 1.5 h and concentrated in vacuo. The residue was dissolved in DCM, washed with saturated NaHCO₃ solution and brine. Following removal of the solvent in vacuo, the residue was subjected to flash column chromatography with EA as the eluent to afford **17** as a slight yellow solid. The preparation of **18** was similar to that of **17**, only with chloroacetyl chloride in place of propionyl chloride. The eluent for the flash column chromatography of **18** was EA/PE/TEA (200:100:3).

4.1.13.1. 6-Bromo-4-((4-(4-propionylpiperazin-1-yl)-3-(trifluoromethyl)phenyl)amino)quinoline-3-carboxamide (17). Light yellow solid; yield: 74% for two steps; ESI-MS: *m/z* = 550 [M+H]⁺.

4.1.13.2. 6-Bromo-4-((4-(4-(2-chloroacetyl)piperazin-1-yl)-3-(trifluoromethyl)phenyl)amino)quinoline-3-carboxamide (18). Light yellow solid; yield: 68% for two steps; ¹H NMR (500 MHz, DMSO-*d*₆): 9.94 (br s, 1H, NH), 8.90 (s, 1H, Ar-H), 8.23 (d, 2.0 Hz, 1H, Ar-H), 8.08 (br s, 1H, NH), 7.92 (d, 9.0 Hz, 1H, Ar-H), 7.89 (dd, 2.0 Hz, 9.0 Hz, 1H, Ar-H), 7.61 (br s, 1H, NH), 7.45 (d, 8.5 Hz, 1H, Ar-H), 7.31 (d, 2.5 Hz, 1H, Ar-H), 7.19 (dd, 2.5 Hz, 8.5 Hz, 1H, Ar-H), 4.44 (s, 2H, Ar-H), 3.65–3.48 (m, 4H, Piperazine-CH₂×2), 2.85 (t, 4.0 Hz, 2H, Piperazine-CH₂), 2.81 (t, 4.0 Hz, 2H, Piperazine-CH₂); ESI-MS: *m/z* = 570 [M+H]⁺.

4.1.14. 6-(6-Aminopyridin-3-yl)-4-((4-(4-propionylpiperazin-1-yl)-3-(trifluoromethyl)phenyl)amino)quinoline-3-carboxamide (19)

The synthetic procedure for compound **19** is according to that of **9a–h**. The eluent for the flash column chromatography of **19** was EA/MeOH/TEA (160:3:2).

Light yellow solid; yield: 59%; $^1\text{H NMR}$ (500 MHz, $\text{DMSO-}d_6$): 10.34 (br s, 1H, NH), 8.91 (s, 1H, Ar-H), 8.20 (br s, 1H, NH), 8.06 (d, 2.5 Hz, 1H, Ar-H), 8.01–7.95 (m, 2H, Ar-H), 7.88 (s, 1H, Ar-H), 7.68 (br s, 1H, NH), 7.51 (d, 8.5 Hz, 1H, Ar-H), 7.47 (dd, 2.5 Hz, 8.5 Hz, 1H, Ar-H), 7.36 (d, 2.5 Hz, 1H, Ar-H), 7.24 (dd, 2.5 Hz, 8.5 Hz, 1H, Ar-H), 6.46 (d, 8.5 Hz, 1H, Ar-H), 6.19 (s, 2H, NH), 3.65–3.48 (m, 4H, Piperazine- $\text{CH}_2 \times 2$), 2.84 (t, 4.5 Hz, 2H, Piperazine- CH_2), 2.80 (t, 4.5 Hz, 2H, Piperazine- CH_2), 2.37 (q, 7.5 Hz, 2H, CH_2), 1.02 (t, 7.5 Hz, 3H, CH_3); ESI-MS: $m/z = 564$ $[\text{M}+\text{H}]^+$; mp 224–226 °C; HPLC: $t_R = 7.11$ min, flow rate 0.9 mL/min, COSMOSIL 5C18-MS-II column (4.6ID \times 250 mm), rt, eluent A-70%, eluent B-30%.

4.1.15. 4'-((4-(2-(4-Methylpiperazin-1-yl)acetyl)piperazin-1-yl)-3-(trifluoromethyl)phenyl)amino)-[3,6'-biquinoline]-3'-carboxamide (20)

To a solution of **18** (1.0 equiv) in anhydrous acetonitrile (10 mL/1 mmol substrate) was added *N*-Methyl piperazine (1.1 equiv) and K_2CO_3 (1.5 equiv). The reaction mixture was allowed to reflux under N_2 atmosphere for 4 h. Afterwards, the solvent was removed in vacuo and the residue was dissolved in DCM, washed with water and brine. Following removal of DCM, the residue was used for the next step without purification. Subsequent Suzuki coupling of the crude product with quinoline-3-boronic acid pinacol ester was carried out according to the general procedure C. The eluent for the flash column chromatography of **20** was EA/MeOH/TEA (20:2:1).

Light yellow solid; yield: 48% for two steps; $^1\text{H NMR}$ (500 MHz, $\text{DMSO-}d_6$): 10.30 (s, 1H, NH), 9.06 (s, 1H, Ar-H), 8.96 (s, 1H, Ar-H), 8.61 (s, 1H, Ar-H), 8.37 (s, 1H, Ar-H), 8.30 (d, 8.5 Hz, 1H, Ar-H), 8.19 (br s, 1H, NH), 8.13 (d, 8.0 Hz, 1H, Ar-H), 8.06 (d, 8.0 Hz, 1H, Ar-H), 8.02 (d, 8.0 Hz, 1H, Ar-H), 7.81–7.78 (m, 1H, Ar-H), 7.73–7.58 (m, 2H, Ar-H, NH), 7.49 (d, 8.5 Hz, 1H, Ar-H), 7.43 (s, 1H, Ar-H), 7.30 (d, 8.5 Hz, 1H, Ar-H), 3.69–3.50 (m, 4H, Piperazine- $\text{CH}_2 \times 2$), 3.29 (s, 2H, CH_2), 3.13–2.96 (m, 2H, Piperazine- CH_2), 2.88–2.77 (m, 4H, Piperazine- $\text{CH}_2 \times 2$), 2.73–2.56 (m, 6H, Piperazine- $\text{CH}_2 \times 3$), 2.36 (s, 3H, CH_3); $^{13}\text{C NMR}$ (125 MHz, $\text{DMSO-}d_6$): δ 169.53, 167.72, 151.04, 149.67, 149.62, 147.40, 147.35, 146.81, 141.26, 134.10, 133.57, 132.46, 130.99, 130.28, 129.98, 129.24, 128.74, 127.95, 127.71, 127.07 ($J_{\text{C-F}} = 27.50$ Hz), 126.14, 124.97, 124.23 ($J_{\text{C-F}} = 272.50$ Hz), 123.49, 121.23, 118.81, 114.98, 60.21, 54.23, 53.53, 51.46, 46.16, 44.67; ESI-MS: $m/z = 683$ $[\text{M}+\text{H}]^+$; mp 211–213 °C; HPLC: $t_R = 11.99$ min, flow rate 0.8 mL/min, COSMOSIL 5C18-MS-II column (4.6ID \times 250 mm), rt, eluent C-80%, eluent B-20%.

4.2. mTOR inhibition assay

mTOR inhibitory activity was assessed by lance ultra assay. mTOR was purchased from Millipore and ATP, DMSO, as well as EDTA were purchased from Sigma. The kinase buffer contained 50 mM HEPES (pH 7.5), 10 mM MgCl_2 , 1 mM EDTA, 3 mM MnCl_2 , 0.01% Tween-20 and 2 mM DTT. The kinase solution was prepared by dissolving the kinase in the kinase buffer and the substrate solution was prepared by dissolving ULight-4E-BP1 peptide substrate and ATP in the kinase reaction buffer. Compound solution, kinase solution and substrate solution were added successively to the

well of the assay plate. The reaction mixture was incubated at room temperature for 1 h, and then stopped by kinase quench buffer containing EDTA and Eu-anti-phospho-4E-BP1 antibody. Before reading on a plate reader, the mixture need be mixed briefly with centrifuge and was allowed to equilibrate for 60 min. The inhibition rate was calculated as $(\text{max} - \text{Lance signal})/(\text{max} - \text{min}) \times 100\%$. Herein, 'max' stands for DMSO control, while 'min' stands for Lance signal of no enzyme control. Finally, data was presented in MS Excel and the curves fitted by Graphpad 5.0. Equation used was: $Y = \text{Bottom} + (\text{Top} - \text{Bottom})/(1 + (\text{IC}_{50}/X)^{\text{HillSlope}})$.

4.3. Cell proliferation assay

Cell proliferation was evaluated by sulforhodamine B (SRB) assay. In detail, HCT116, PC3 and MCF-7 cells were seeded into 96-well plates, cultured overnight and then exposed to serial concentrations of compounds for 72 h. Subsequently, cells were washed with PBS and fixed with 10% (w/v) trichloroacetic acid at 4 °C for 1 h. Afterwards, the cells were stained for 30 min with 0.4% SRB dissolved in 1% acetic acid. Then the cells were washed by 1% acetic acid for 5 times, and protein-bound dye was extracted with 10 mmol unbuffered Tris base. The absorbance was measured at 515 nm using a multiscan spectrum (Thermo Electron Co., Vantaa, Finland). The inhibition rate on proliferation of each well was calculated as $(\text{A515 control cells} - \text{A515 treated cells})/\text{A515 control cells} \times 100\%$. The average IC_{50} values were determined by Logit method from at least two independent tests.

4.4. Class I PI3Ks selectivity assay

PI3K α inhibitory activity was assessed by Kinase-Glo Luminescent assay. PI3K α was purchased from Invitrogen and ATP, DMSO, as well as EDTA were purchased from Sigma. The kinase buffer contained 50 mM HEPES (pH 7.5), 3 mM MgCl_2 , 1 mM EDTA, 100 mM NaCl, 0.03% CHAPS and 2 mM DTT. The kinase solution was prepared by dissolving the kinase in the kinase buffer and the substrate solution was prepared by dissolving PIP_2 and ATP in the kinase reaction buffer. Compound solution, kinase solution and substrate solution were added successively to the well of the assay plate. The reaction mixture was incubated at room temperature for 1 h, and then stopped by Kinase-Glo reagent. Before reading on a plate reader for luminescence, the mixture need be mixed briefly with centrifuge and was allowed to equilibrate for 15 min. The percent inhibition was calculated as $100 - (\text{max} - \text{sample RLU})/(\text{max} - \text{min}) \times 100$. Herein, 'max' stands for the RLU of no enzyme control, while 'min' means the RLU of DMSO control. Finally, data was presented in MS Excel and the curves fitted by Graphpad 5.0. Equation used was: $Y = \text{Bottom} + (\text{Top} - \text{Bottom})/(1 + (\text{IC}_{50}/X)^{\text{HillSlope}})$.

PI3K β inhibitory activity was assessed by ADP-Glo Luminescent assay. PI3K β was purchased from Millipore and ATP, DMSO, as well as EDTA were purchased from Sigma. The kinase reaction mixture was incubated at room temperature for 1 h. Afterwards, a little amount of reaction mixture was transferred to a new 384 plate and equal amount of ADP-Glo reagent was added to each well of the new assay plate to stop the reaction. After being mixed briefly with centrifuge, the resultant mixture was shaken slowly on the shaker and equilibrated for 40 min. Kinase detection reagent was then added to each wells. The mixture was shaken 1 min, equilibrated for 60 min before reading on a plate reader for luminescence. The percent inhibition was calculated as $(\text{max} - \text{sample RLU})/(\text{max} - \text{min}) \times 100$. Herein, 'max' stands for the RLU of DMSO

control, while 'min' means the RLU of no enzyme control. Finally, data was presented in MS Excel and the curves fitted by Graphpad 5.0. Equation used was: $Y = \text{Bottom} + (\text{Top} - \text{Bottom}) / (1 + (\text{IC}_{50}/X)^{\text{HillSlope}})$. PI3K γ and δ inhibitory activities were evaluated according to the PI3K β inhibition assay.

4.5. Western blot analysis

Cells were treated with final concentrations of 0.1 μM or 0.5 μM of BEZ235, rapamycin, compound **16b** and DMSO, and incubated at 37 $^{\circ}\text{C}$ for 2 h. Afterwards, cells were washed twice with ice-cold PBS and cell lysis buffer was added. Then the cellular debris was pelleted by centrifugation at 13,000 rpm for 30 min at 4 $^{\circ}\text{C}$ and the supernatant was collected. For western blot analysis, the proteins were separated on SDS-PAGE and then transferred onto PVDF membrane. The membranes were incubated with antibodies against pS6(Ser235) (Cell Signaling Technology), pAkt(Ser473) (Cell Signaling Technology) and GAPDH (Santa Cruz), washed by PBST and then incubated with secondary antibodies. Finally, proteins were visualized using enhanced chemiluminescence.

4.6. In vitro stability assay

The in vitro stability in SGF, SIF and liver microsome was evaluated according to the reported assay with some modification.²⁴

4.7. Molecular docking

The co-crystal structure of mTOR in complex with Torin 2 (PDB code 4JSX) was used for the docking calculation in C-DOCKER module (Discovery Studio, version 2.5; Accelrys, San Diego, CA, USA, 2008). After removal of Torin 2 and solvent molecules, the CHARMM-force field was applied to the protein. The active site was determined according to the location of Torin 2 in mTOR enzyme and each ligand was docked into the defined site. The final binding conformations of them were determined based on the calculated CDOCKING ENERGE.

Acknowledgments

The authors thank Jianyang Pan (Institute of Pharmaceutical Informatics, Zhejiang University, China) for performing NMR spectrometry and mass spectrometry for structural characterization.

References and notes

- Sabbah, D. A.; Brattain, M. G.; Zhong, H. *Curr. Med. Chem.* **2011**, *18*, 5528.
- Nowak, P.; Cole, D. C.; Brooijmans, N.; Bursavich, M. G.; Curran, K. J.; Ellingboe, J. W.; Gibbons, J. J.; Hollander, I.; Hu, Y.; Kaplan, J.; Malwitz, D. J.; Toral-Barza, L.; Verheijen, J. C.; Zask, A.; Zhang, W. G.; Yu, K. *J. Med. Chem.* **2009**, *52*, 7081.
- Ma, X.; Hu, Y. *Curr. Med. Chem.* **2013**, *20*, 2991.
- Chresta, C. M.; Davies, B. R.; Hickson, I.; Harding, T.; Cosulich, S.; Critchlow, S. E.; Vincent, J. P.; Ellston, R.; Jones, D.; Sini, P.; James, D.; Howard, Z.; Dudley, P.; Hughes, G.; Smith, L.; Maguire, S.; Hummersone, M.; Malagu, K.; Menear, K.; Jenkins, R.; Jacobsen, M.; Smith, G. C.; Guichard, S.; Pass, M. *Cancer Res.* **2010**, *70*, 288.
- Sarbasov, D. D.; Ali, S. M.; Sengupta, S.; Sheen, J. H.; Hsu, P. P.; Bagley, A. F.; Markhard, A. L.; Sabatini, D. M. *Mol. Cell* **2006**, *22*, 159.
- O'Reilly, K. E.; Rojo, F.; She, Q. B.; Solit, D.; Mills, G. B.; Smith, D.; Lane, H.; Hofmann, F.; Hicklin, D. J.; Ludwig, D. L.; Baselga, J.; Rosen, N. *Cancer Res.* **2006**, *66*, 1500.
- Koehler, M. F.; Bergeron, P.; Blackwood, E.; Bowman, K. K.; Chen, Y. H.; Deshmukh, G.; Ding, X.; Epler, J.; Lau, K.; Lee, L.; Liu, L.; Ly, C.; Malek, S.; Nonomiya, J.; Oeh, J.; Ortwine, D. F.; Sampath, D.; Sideris, S.; Trinh, L.; Truong, T.; Wu, J.; Pei, Z.; Lyssikatos, J. P. *J. Med. Chem.* **2012**, *55*, 10958.
- Lane, H. A.; Breuleux, M. *Curr. Opin. Cell Biol.* **2009**, *21*, 219.
- Favre, S.; Kroemer, G.; Raymond, E. *Nat. Rev. Drug Disc.* **2006**, *5*, 671.
- Liu, Q.; Wang, J.; Kang, S. A.; Thoreen, C. C.; Hur, W.; Ahmed, T.; Sabatini, D. M.; Gray, N. S. *J. Med. Chem.* **2011**, *54*, 1473.
- Zheng, B.; Mao, J. H.; Qian, L.; Zhu, H.; Gu, D. H.; Pan, X. D.; Yi, F.; Ji, D. M. *Cancer Lett.* **2015**, *357*, 468.
- Huo, H. Z.; Zhou, Z. Y.; Wang, B.; Qin, J.; Liu, W. Y.; Gu, Y. *Biochem. Biophys. Res. Commun.* **2014**, *443*, 406.
- Liu, Q.; Thoreen, C.; Wang, J.; Sabatini, D.; Gray, N. S. *Drug Discovery Today Ther. Strategies* **2009**, *6*, 47.
- Stauffer, F.; Maira, S. M.; Furet, P.; Garcia-Echeverria, C. *Bioorg. Med. Chem. Lett.* **2008**, *18*, 1027.
- Bowles, D. W.; Jimeno, A. *Expert Opin. Invest. Drugs* **2011**, *20*, 507.
- Maira, S. M.; Stauffer, F.; Brueggen, J.; Furet, P.; Schnell, C.; Fritsch, C.; Brachmann, S.; Chene, P.; De Pover, A.; Schoemaker, K.; Fabbro, D.; Gabriel, D.; Simonen, M.; Murphy, L.; Finan, P.; Sellers, W.; Garcia-Echeverria, C. *Mol. Cancer Ther.* **2008**, *7*, 1851.
- Knight, S. D.; Adams, N. D.; Burgess, J. L.; Chaudhari, A. M.; Darcy, M. G.; Donatelli, C. A.; Luengo, J. L.; Newlander, K. A.; Parrish, C. A.; Ridgers, L. H.; Sarpong, M. A.; Schmidt, S. J.; Van Aller, G. S.; Carson, J. D.; Diamond, M. A.; Elkins, P. A.; Gardiner, C. M.; Garver, E.; Gilbert, S. A.; Gontarek, R. R.; Jackson, J. R.; Kershner, K. L.; Luo, L.; Raha, K.; Sherk, C. S.; Sung, C. M.; Sutton, D.; Tummino, P. J.; Wegrzyn, R. J.; Auger, K. R.; Dhanak, D. *ACS Med. Chem. Lett.* **2010**, *1*, 39.
- Markman, B.; Atzori, F.; Perez-Garcia, J.; Tabernero, J.; Baselga, J. *Ann. Oncol.* **2010**, *21*, 683.
- Wu, P.; Hu, Y. Z. *Curr. Med. Chem.* **2010**, *17*, 4326.
- Cheng, H. M.; Bagrodia, S.; Bailey, S.; Edwards, M.; Hoffman, J.; Hu, Q. Y.; Kania, R.; Knighton, D. R.; Marx, M. A.; Ninkovic, S.; Sun, S. X.; Zhang, E. *Medchemcomm* **2010**, *1*, 139.
- Liu, Q.; Wang, J.; Kang, S. A.; Thoreen, C. C.; Hur, W.; Choi, H. G.; Waller, D. L.; Sim, T.; Sabatini, D. M.; Gray, N. S. *Bioorg. Med. Chem. Lett.* **2011**, *21*, 4036.
- Yang, H.; Rudge, D. G.; Koos, J. D.; Vaidialingam, B.; Yang, H. J.; Pavletich, N. P. *Nature* **2013**, *497*, 217.
- Lin, A. J.; Loo, T. L. *J. Med. Chem.* **1978**, *21*, 268.
- Zhou, H. J.; Aujay, M. A.; Bennett, M. K.; Dajee, M.; Demo, S. D.; Fang, Y.; Ho, M. N.; Jiang, J.; Kirk, C. J.; Laidig, G. J.; Lewis, E. R.; Lu, Y.; Muchamuel, T.; Parlati, F.; Ring, E.; Shenk, K. D.; Shields, J.; Shwonek, P. J.; Stanton, T.; Sun, C. M.; Sylvain, C.; Woo, T. M.; Yang, J. *J. Med. Chem.* **2009**, *52*, 3028.